NACA

RESEARCH MEMORANDUM

ANALYTICAL DETERMINATION OF EFFECT OF TURBINE COOLING-

AIR-IMPELLER PERFORMANCE ON ENGINE PERFORMANCE

AND COMPARISON OF EXPERIMENTALLY DETERMINED

PERFORMANCE OF IMPELLERS WITH AND

WITHOUT INDUCER VANES

By Louis J. Schafer, Jr. and Robert O. Hickel

Lewis Flight Propulsion Laboratory
Cleveland, Ohio

NATIONAL ADVISORY COMMITTEE
FOR AERONAUTICS

WASHINGTON

October 25, 1954
Declassified August 16, 1956

H

NATIONAL ADVISORY COMMITTEE FOR AERONAUTICS

RESEARCH MEMORANDUM

ANALYTICAL DETERMINATION OF EFFECT OF TURBINE COOLING-AIR-IMPELLER

PERFORMANCE ON ENGINE PERFORMANCE AND COMPARISON OF EXPERIMENTALLY

DETERMINED PERFORMANCE OF IMPELLERS WITH AND WITHOUT INDUCER VANES

By Louis J. Schafer, Jr. and Robert O. Hickel

SUMMARY

The effects of cooling-air-impeller performance on turbojet-engine performance were determined analytically for operation at 70 and 100 percent of rated engine speed. A turbine cooling-air impeller having straight radial impeller vanes (no inlet inducer section) was investigated experimentally at engine speeds to 70 percent of the rated condition.

The analysis indicated that impeller performance has little effect on engine performance at rated engine speed for the coolant flows considered. At this speed, increasing the required impeller-inlet total pressure from 50 to 100 percent of the available compressor-exit total pressure (decreasing impeller performance) decreased engine thrust about 1 percent and increased specific fuel consumption about 1.3 percent at a coolant-flow ratio of 0.03. At a coolant-flow ratio of 0.05, the decrease in specific thrust was 1.8 percent and the increase in specific fuel consumption was 1.9 percent. The effects are greater at 70 percent of rated speed.

The experimental results showed that the impeller had about the same relative total-pressure ratio as a previously reported impeller with an inducer section. Either impeller could supply tube-filled nonstrategic turbine blades with about three times as much cooling air as is required for operation at current turbine-inlet temperatures.

Since impellers with and without inducer sections had essentially the same pressure ratios and the engine performance was not extremely sensitive to impeller performance for coolant-flow ratios up to 0.05 at rated engine speed, it is unnecessary to complicate the impeller fabrication by including an inducer section at the impeller-vane inlet.

INTRODUCTION

Turbine cooling permits engine operation at elevated gas-temperature levels where gains in engine performance can be realized (refs. 1 and 2). The application of turbine cooling requires some type of impeller to distribute the cooling air uniformly to all the turbine blades and at the same time give some pressure rise to the cooling air to overcome the friction pressure losses in the turbine blades and in the cooling-air system between the compressor and the turbine blade tips.

One cooling-air-impeller design incorporating an inducer at the impeller inlet was investigated in reference 3. The results indicate that the impeller could supply sufficient cooling air to cool nonstrategic tube-filled blades at present-day gas temperatures or blades made of a strategic material at higher gas temperatures.

Because the impeller pressure-ratio results of reference 3 include the effects of the pressure losses in the turbine blades, the pressure ratio of the impeller alone was unknown. Consequently, the efficiency of the impeller was not determined. It can be shown, however, that even for efficiencies of 100 percent the pressure rise through cooling-air impellers for current engines would not be large, because the tangential speed at the outlet of the impeller is relatively low. Furthermore, the pressure available at the exit of the impeller for forcing air through the turbine blades is relative to the rotor. Although low cooling-air-impeller pressure ratios are to be expected, no study has previously been made of the effect of impeller pressure ratio on engine performance. Also, the degree to which impeller passage fabrication can be simplified (e.g., by eliminating the inducer vanes) and still supply sufficient cooling air to the turbine blades was not known.

The purposes of this report are:

(1) To investigate analytically the effects of impeller performance on the performance of a typical turbojet engine

(2) To determine experimentally the pressure ratio of a straight radial-vaned impeller (no inducer vanes) and compare its performance with that of an impeller with an inducer section (ref. 3)

(3) To determine analytically whether a straight-vaned impeller that would operate at a high or unfavorable angle of incidence would permit the compressor to supply sufficient cooling air to cool nonstrategic tube-filled blades at present turbine-inlet temperatures or strategic blades at higher temperatures

The turbine blades of reference 3 were of a different internal configuration from the blades used in the present investigation; consequently, they would be expected to have different cooling-air pressure losses. In order to eliminate the effects on impeller performance of the air-cooled turbine blade configuration and thus eliminate the cooling-air pressure loss within the blades, the impeller performance of reference 3 and of this report must be compared on the basis of pressure rise through the impeller alone. To do so, a static calibration of the blade pressure losses was made, the details of which are presented in appendix B. (Symbols are defined in appendix A.)

The analysis was made for a centrifugal-compressor turbojet engine at sea-level static conditions for engine speeds of 8000 and 11,500 rpm. The experimental investigations were made at engine speeds of 4000, 6000, and 8000 rpm for a range of coolant-flow ratio from 0.02 to 0.11. The design speed of the engine was 11,500 rpm, but this investigation was limited to 8000 rpm by low aerodynamic performance of the turbine blades, which resulted in high turbine-inlet temperatures and in turn caused premature surging of the compressor at engine speeds slightly above 8000 rpm.

APPARATUS

Engine Modifications

The modified air-cooled turbojet engine used in this investigation was the same as that described in detail in references 3 to 5, with the exception of the turbine disk and blades. The modifications made to supply cooling air to the turbine are shown in figure 1 and are discussed in detail in reference 5. This report is concerned specifically with a modification of the turbine disk and blades.

Turbine rotor. - A split-disk air-cooled turbine rotor with cooling air entering from the downstream side of the rotor was employed in this investigation. The rotor was split along the center line in the plane of rotation and had individual passages to each blade machined into the inside surface of each half of the disk to form the vane system shown in figure 2(a). The vane system incorporated in the split disk investigated in references 3 and 4 is shown in figure 2(b). In order to simplify fabrication of the disk investigated in the present report, the knee or break in the vanes, which forms the inducer section of the rotor shown in figure 2(b), was eliminated. The detailed geometry and dimensions of the two types of impeller are shown in figure 3.

The rotor with no inducer section (fig. 2(a)) was made from two forged disk halves, and the axial thickness of this rotor was the same as that of a standard uncooled rotor. The rotor with the inducer section (fig. 2(b)) was made by splitting a standard uncooled rotor in the

plane of rotation, which resulted in a total axial thickness about 1/2 inch less than that of a standard uncooled rotor (ref. 3). Because of this difference in axial thickness, the bases of the blades for the present investigation were longer axially than those used in references 3 and 4. As a result, the axial divergence in the cooling-air passages within the rotor near the rim was greater for the rotor without the inducer section than for the rotor with the inducer (fig. 3).

Turbine blades. - Photographs of one of the nontwisted air-cooled turbine blades of this investigation and one of those of reference 3 are compared in figure 4. Both blades had small tubes installed in the blade shell to increase the internal cooling surface area. The detailed fabrication procedures for cooled blades made by the NACA are given in reference 6. The end view of the blades (fig. 4) shows that, even though the blades were the same type, the geometry of the two blade profiles was different. Also, the lack of divergence in the cooling-air passage through the base of the blade of this investigation permitted the tubes in the cooling-air passage to extend through the blade base. In the blade of reference 3 the tubes terminated at the divergent section in the blade base.

Instrumentation

Engine. - The engine speed was measured with a chronometric tachometer. The mass flow of air through the compressor was calculated from temperature and pressure measurements made in a venturi installed in the duct supplying air to the sealed test cell. The total pressure at the compressor exit was measured with three total-pressure probes in the diffusers between the compressor exit and the combustors. Fuel flow was measured by means of calibrated rotameters. Two static-pressure taps were located 180° apart in the outer tail-cone casing directly over the midchord region of the coolant passages of the rotor blades (fig. 1) to determine the static pressure of the combustion gases in the region of the cooling-air discharge.

Cooling air. - The cooling-air flow to the turbine rotor was controlled remotely by valves and was measured by a standard A.S.M.E. flat-plate orifice installed in the cooling-air supply system upstream of the tail cone. The temperature of the cooling air at the turbine impeller inlet was measured with two iron-constantan thermocouples on the survey rake in the cooling-air supply tube (fig. 1). The cooling-air temperature at the impeller exit was measured with three chromel-alumel thermocouples, one installed in the cooling-air passage in the base of each of three of the turbine blades. These thermocouples were located immediately upstream of the small cooling-air tubes in the blades. The cooling-air total pressure at the impeller inlet was measured with three total-pressure probes mounted on the rake at the impeller inlet.

Turbine blades. - The temperature of three of the turbine blade
shells was measured with three thermocouples on each of the blades, on
a plane about one-third of the blade span from the base. On each blade
a thermocouple was located at the leading edge, the midchord on the pres-
sure surface, and the trailing edge.

EXPERIMENTAL PROCEDURE

The performance of the cooling-air impeller was obtained by operat-
ing the engine at three nominal constant impeller speeds of 4000, 6000,
and 8000 rpm. At each of these speeds, the coolant-flow rate was varied
by changing the pressure at the impeller inlet. At each coolant flow,
the following data were taken: total temperature at stations 6 and 7
(figs. 5 and 6), total pressure at station 6, and static pressure at
station 10.

CALCULATION PROCEDURES

Variation of Engine Performance with Impeller Pressure Ratio

An analysis was made for sea-level static conditions for a current
turbojet engine at two engine speeds (70 and 100 percent of rated) to
determine the effect of impeller performance on engine thrust and spe-
cific fuel consumption. The following general assumptions are made in
the analysis for each constant engine speed:

(1) The corrected combustion-gas flow at station 3, $w_3\sqrt{\theta_3}/\delta_3$, is
constant.

(2) Air weight flow into the engine w_1 is constant.

(3) Turbine-inlet total temperature T_3' is constant.

(4) Combustion efficiency, compressor efficiency, and turbine ef-
ficiency do not vary with cooling-air flow or impeller pressure ratio.

(5) Five percent of the compressor-exit total pressure is lost in
the combustor.

(6) There is no combustion-gas total-temperature or pressure loss
in the engine tail pipe between the turbine exit and tail-pipe nozzle
(stations 4 to 5).

(7) The tail-pipe nozzle coefficient is 1.0.

In order to make the analysis it is necessary to assign values of
pressure, temperature, air flow, and gas flow at certain points in the

engine. The values used in the analysis for the two engine speeds se-
lected are listed in the following table and are based on values ob-
tained from unpublished data on a typical current turbojet engine:

	Engine speed, rpm	
	8000	11,500
Corrected compressor-inlet weight flow, $w_1\sqrt{\theta_1}/\delta_1$, lb/sec	47.0	75.7
Compressor efficiency, η_C	0.80	0.80
Turbine efficiency, η_T	0.80	0.80
Corrected combustion-gas flow at stator inlet, $w_3\sqrt{\theta_3}/\delta_3$, lb/sec	41.0	41.0
Turbine-inlet total temperature, T_3', °R	1480	2110
Combustion-gas absolute static pressure at blade tips, p_{10}, in. Hg abs	34.6	50.0

The general procedure for determining the variation of engine
thrust and specific fuel consumption with impeller pressure ratio at a
constant coolant flow is as follows: For a given cooling-air flow, a
range of required cooling-air total pressure at the impeller inlet is
chosen to represent varying impeller performance. Then, with the as-
sumed turbine-inlet total temperature T_3', turbine weight flow w_3, and
corrected turbine weight flow $w_3\sqrt{\theta_3}/\delta_3$, the total pressure of the gas
at the turbine inlet is determined. The power output of the turbine is
then calculated and is used with the turbine-inlet conditions to give
the combustion-gas conditions downstream of the turbine. These condi-
tions are then used to obtain the engine thrust.

The turbine power consists of the power required to drive the com-
pressor plus the power expended on the cooling air in passing through
the turbine disk and blades. The power to drive the compressor is
expressed by the equation

$$\Omega_C = \frac{w_1 - w_a}{\eta_C} c_p T_1' \left[\left(\frac{p_2'}{p_1'}\right)^{\frac{\gamma-1}{\gamma}} - 1\right] + \frac{w_a}{\eta_C} T_1' c_p \left[\left(\frac{p_{2,a}'}{p_1'}\right)^{\frac{\gamma-1}{\gamma}} - 1\right]$$

$$(1)$$

and the power expended on the cooling air in the turbine rotor is

$$\Omega_a = w_a \frac{\omega^2 r_9^2}{gJ} \tag{2}$$

The sum of equations (1) and (2) is the power output of the turbine Ω_T.

The values of p_2'/p_1' and $p_{2,a}'/p_1'$ must be evaluated before the power expressed by equation (1) can be calculated. This is done as follows: The value of $\delta_3 = p_3'/p_1'$ is calculated using the assumed constant value of $w_3 \sqrt{\theta_3}/\delta_3$ with the assumed constant value of θ_3 and w_3 from the relation

$$w_3 = w_1 \left[1 + f\left(1 - \frac{w_a}{w_1}\right) - \frac{w_a}{w_1} \right] \tag{3}$$

where values of w_1 and w_a/w_1 are assumed. The value of p_2'/p_1' is then obtained from δ_3 by assuming a 5-percent total-pressure loss through the combustors. Since the value of p_1' is known and $p_{2,a}'$ is assumed equal to p_6', the values of $p_{2,a}'/p_1'$ can be computed for the range of assumed impeller performance. The value of the coolant flow w_a is the product of the constant compressor-inlet air flow and the assumed value of w_a/w_1.

The gas total pressure downstream of the turbine is obtained as follows: The turbine power can be expressed as

$$\Omega_T = w_3 \, c_{p,3} \, \eta_T \, T_3' \left[1 - \left(\frac{p_4'}{p_3'}\right)^{\frac{\gamma_3-1}{\gamma_3}} \right] \tag{4}$$

and as

$$\Omega_T = w_3 \, c_{p,3} \left(T_3' - T_4' \right) \tag{5}$$

Equation (4) is solved for the turbine total-pressure ratio p_3'/p_4', and equation (5) for T_4'. This gives the combustion-gas conditions downstream of the turbine. The value of p_5' is assumed equal to p_4', and p_5 is equal to p_1 for the sea-level static condition assumed in this analysis. The temperature of the mixture of cooling air and combustion gas at station 5 (T_5') is obtained from the equation

$$w_5 h_5' = w_4 h_4' + w_a \left(h_6' + \frac{\omega^2 r_9^2}{gJ} \right) \tag{6}$$

where $w_4 = w_3$. (It is assumed that the cooling air has not yet mixed with the combustion gas at station 4.) The jet velocity out the tail pipe can then be calculated as follows:

$$V_5 = \left\{ \frac{2\gamma_5}{\gamma_5 - 1} \, gRT_5' \left[1 - \left(\frac{p_5}{p_5'} \right)^{\frac{\gamma_5 - 1}{\gamma_5}} \right] \right\}^{\frac{1}{2}} \tag{7}$$

and the engine thrust for sea-level static conditions is

$$F = \frac{w_1 + w_F}{g} \, V_5 \tag{8}$$

where

$$w_F = w_1 f \left(1 - \frac{w_a}{w_1} \right) \tag{9}$$

The specific fuel consumption is defined as w_F/F. Over-all rotor adiabatic efficiencies from the impeller inlet to the turbine blade tips are calculated with the equation

$$\eta_R = \frac{c_p \, T_6' \left[\left(\frac{p_9''}{p_6'} \right)^{\frac{\gamma_6 - 1}{\gamma_6}} - 1 \right]}{\frac{\omega^2 r_9^2}{2gJ}} \tag{10}$$

where T_6' is fixed by the compressor stage from which the cooling air is bled to give the assumed total pressure at the impeller inlet p_6'. The value of p_9'' is calculated with the values of p_{10}, w_a, A_b, and T_9'' and the continuity equation. The value of A_b is the cooling-air flow area of the turbine blade used with the impeller without inducer vanes (fig. 4(a)). The temperature at the blade tip T_9'' is obtained with values calculated from the engine data as described in the next section.

Blade Pressure Loss and Impeller Pressure Ratio

The total pressure at the exit from the rotating cooling-air impeller could not be measured, because rotating pressure-measuring instrumentation is not currently available. Therefore, the total pressure at the impeller exit must be determined from the measured conditions at the tips of the turbine blades. This calculation is made in the following steps:

(1) The total pressure of the cooling air at the blade tips is calculated from the measured static pressure at station 10 (fig. 6), the total temperature at station 9, the blade coolant-flow area, and the coolant flow.

(2) The coolant-passage total-pressure loss is calculated with the use of the charts of reference 7.

(3) The total-pressure loss across the blade base is calculated with the contraction loss coefficient determined in the pressure-loss calibration rig as described in appendix B.

(4) The pressure loss through the blade cooling-air passage and through the blade base is added to the total pressure at the blade tip to obtain the cooling-air total pressure at the exit of the cooling-air impeller.

The calculation procedure used to determine the turbine blade pressure losses for both the turbine rotor of this report and the rotor of reference 3 is generally the same as outlined in appendix B. However, the calculations for the engine data require some additional operations because of heat transfer to the cooling air in the turbine blades and rotation of the turbine blades. Only the points where the procedure differs from that of appendix B are discussed here.

The following four parameters must be evaluated before the pressure-loss charts of reference 7 can be used to evaluate the cooling-air pressure loss through the turbine blades in the engine investigation:

$$(1) \ M_9 \qquad\qquad\qquad (3) \ \frac{4 f r_K (r_9 - r_8)}{D_h}$$

$$(2) \ \frac{T_9''}{T_8''} \qquad\qquad\qquad (4) \ \frac{\omega^2 r_9 (r_9 - r_8)}{T_9''}$$

The cooling-air flow area through the turbine blades used in the calculation of the cooling-air Mach number at the blade tip M_9 in the

calibration rig is the measured blade flow area at the tip. However, in
the engine investigation the blade flow area varied from blade to blade
because of the different degrees of area blockage resulting from the
variation of the amount of braze material flowing into the cooling-air
passages during blade fabrication. Since an accurate evaluation of the
average flow area for all the blades on the rotor could not be made, it
is assumed that there was zero area blockage of the cooling-air passages
for both the turbine blade configurations considered herein. This as-
sumption results in some error in the calculation of the blade cooling-
air pressure loss; but, since the same assumption is made for both sets
of blades, the relative magnitudes of the blade pressure losses for both
should be essentially correct, and the resulting impeller pressure ratios
should be comparable.

When heat is transferred to the cooling air, the ratio of exit to
inlet cooling-air total temperature must be known to use the pressure-
loss charts of reference 7. In a rotating turbine blade, the cooling-
air temperature rise from root to tip is the sum of the temperature rise
resulting from rotation and that resulting from heat transfer. The tem-
perature rise resulting from rotation is

$$\Delta T_R'' = \frac{\omega^2(r_9^2 - r_8^2)}{2gJc_p} \tag{11}$$

and that due to heat transfer is

$$\Delta T_H'' = \frac{\overline{h}_f S \left(\overline{T}_b - \overline{T}_a''\right)}{w_a c_p} \tag{12}$$

The value of $\overline{h}_f$ in this equation is obtained from equation (6) of
reference 8 (notation of this report):

$$\overline{h}_f = \frac{\overline{h}_{a,b}}{m+\tau} \left(\frac{2L \tanh L\varphi}{L\varphi} + m\right) \tag{13}$$

A detailed discussion of the application of this equation to tube-filled
air-cooled turbine blades is given in reference 9, where the value of
$\overline{h}_{a,b}$ is obtained from

$$\overline{h}_{a,b} = 0.019(\mathrm{Re}_{a,b})^{0.8} \left(\frac{\overline{k}_{a,b}}{D_h}\right) \tag{14}$$

where

$$Re_{a,b} = \frac{w_a \, D_h}{A_b \, \mu_{a,b} \, g} \left(\frac{\overline{T}_a''}{\overline{T}_b} \right) \tag{15}$$

In this equation the value of $\overline{T}_b$ is obtained from the engine data. The value of $\overline{T}_a''$ in equations (12) and (15) is obtained by an iteration process. The value of T_9'' can then be obtained as

$$T_9'' = T_8'' + \Delta T_R'' + \Delta T_H'' \tag{16}$$

Thus, with this temperature of the cooling air at the tip of the turbine blades, the cooling-air flow area, the cooling-air weight flow, and the measured static pressure at station 10, the cooling-air Mach number at the blade tips can be determined. Then T_9'' and the measured value of T_8'' are used to obtained the temperature ratio T_9''/T_8''.

The friction factor, corrected for entrance effect as described in appendix B, for the evaluation of the parameter $4fr_K(r_9 - r_8)/D_h$ is obtained from the von Kármán friction-factor equation, which is also discussed in appendix B. Because of the presence of heat transfer in the engine investigation, the Reynolds number used in the determination of the friction factor is evaluated from the film temperature between the cooling air and the blade shell. Reference 10 shows that the friction factor can be correlated fairly well with Reynolds number for various rates of heat transfer when the Reynolds number is thus evaluated. Therefore, the Reynolds number becomes

$$Re_{film} = \frac{w_a}{A_b} \frac{D_h}{\mu_{film} \, g} \frac{\overline{T}_a''}{T_{film}} \tag{17}$$

The cooling-air total-pressure loss from stations 8 to 9 is determined from the procedure outlined in appendix B and from the additional information given herein to cover the conditions of heat transfer and rotation.

The value of the parameter $\omega^2 r_9 (r_9 - r_8)/T_9''$ is obtained from known measurements and equation (16).

The cooling-air total-pressure loss across the turbine blade base (stations 7 to 8) is determined in the engine investigation by exactly the same procedure as presented in appendix B for the pressure-loss calibration rig. No pressure rise across the blade base resulting from rotation is considered, because the difference in rotor diameter between these stations is small. Thus,

$$\frac{p_7'' - p_8''}{p_8} = K \left(\frac{w_a^2 T_8}{A_8^2 p_8^2}\right) \frac{R}{2g} \tag{18}$$

The relative total pressure at the impeller exit is

$$p_7'' = p_9'' + \Delta p_{8-9}'' + \Delta p_{7-8}'' \tag{19}$$

The ratio of this relative total pressure at the impeller exit (station 7) to the measured total pressure at the impeller inlet (station 6) gives the impeller relative total-pressure ratio. A calculation such as this is made for both the impeller of this investigation and the impeller of reference 3 to provide a basis for comparing performance.

Cooling Air Available with Compressor Bleed

The turbine-cooling air will probably be bled from the compressor in a production turbojet engine. Therefore, the maximum pressure available at the inlet to the cooling-air impeller is limited to a value equal to the compressor-exit total pressure minus the ducting pressure losses between the compressor and the turbine hub. The following assumptions are made in determining the impeller range of operation with air bled from the compressor exit:

(1) Available total pressure at the turbine hub is equal to the compressor-exit total pressure.

(2) Cooling-air total-pressure loss through the turbine blade used with the cooling-air impellers in this calculation is the same as that through the blades used on the impeller without inducer vanes in the experimental investigation.

This calculation is made for an engine speed of 8000 rpm, since this is the highest engine speed for which experimental impeller data were obtained in the present investigation. The required total pressure at the base of the turbine blades for a given cooling-air weight flow is obtained from the calculations of the blade pressure loss needed in the evaluation of the experimental impeller pressure ratio. This required total pressure at the base of the blade corresponds to the impeller-exit pressure. With the use of this required total pressure, the impeller pressure ratios of the two impellers of this report, and the hypothetical 100-percent-efficient impeller, the total pressure required at the impeller inlet can be determined for a range of coolant flows. The percentage of the compressor-exit total pressure at this engine speed corresponding to the required impeller-inlet total pressures can also be calculated.

The total-pressure ratio across an impeller having an adiabatic efficiency of 100 percent is calculated with the equation

$$\frac{p_7''}{p_6'} = \left(1 + \frac{\omega^2 r_7^2}{2gJc_p T_6'}\right)^{\frac{\gamma}{\gamma-1}} \tag{20}$$

RESULTS AND DISCUSSION

Whether or not there is a need for a high-performance cooling-air impeller should be determined by evaluating the effect of the impeller performance on the engine performance (thrust and specific fuel consumption) and also the effect of impeller performance on the maximum cooling-air flow that can be forced through the turbine blades when the cooling air is bled from the compressor.

Effect of Impeller Performance on Engine Performance

A low-performance cooling-air impeller requires a higher cooling-air supply pressure at its inlet for a given cooling-air flow than a high-performance impeller. This means that for the low-performance impeller the cooling air must be bled from a later stage of the compressor. Thus, it is necessary that the turbine expend more power to drive the compressor, and the resulting extraction of more energy from the combustion-gas stream decreases the engine thrust and increases the specific fuel consumption.

Calculations were made to determine the effect of impeller performance on engine thrust and specific fuel consumption by determining the engine performance for a series of assumed cooling-air supply total pressures required at the impeller inlet for a constant cooling-air flow. These calculations were made for the maximum engine speed attained in the impeller investigation of this report (8000 rpm) and for rated engine speed (11,500 rpm) at coolant-flow ratios w_a/w_1 of 0.03 and 0.05. The results of the calculations for 8000 rpm are presented in figure 7(a). When the required total pressure at the impeller inlet is increased from 50 to 100 percent of the compressor-exit total pressure at a coolant-flow ratio of 0.03, the engine specific thrust decreases from 27.2 to 25.9 pound-seconds per pound (4.8 percent), corresponding to a 60-pound loss in total engine thrust. The same change in required impeller-inlet total pressure at a coolant-flow ratio of 0.05 results in a decrease in engine specific thrust from 25.5 to 23.2 pound-seconds per pound (9 percent), corresponding to a 100-pound loss in total engine thrust. For the same increase in impeller-inlet pressure, the thrust specific fuel consumption increases from 1.53 to 1.61 lb/(hr)(lb) at a coolant-flow ratio of 0.03

and from 1.61 to 1.77 lb/(hr)(lb) at a coolant-flow ratio of 0.05 (increases of 5.2 and 9.9 percent, respectively). Since the cruise speed of an engine is usually greater than 70 percent of rated, the effects of impeller performance on engine performance at cruise speed will be smaller than those shown in figure 7(a).

The lines of constant over-all rotor adiabatic efficiency η_R shown in figure 7(a) represent an efficiency calculated on the basis of the over-all total-pressure ratio from the blade exit to the impeller inlet. Since these efficiencies include the turbine blade pressure loss, it is possible to have a pressure ratio from the turbine blade tip to impeller inlet that is less than 1.0. Such pressure ratios result in the negative values of over-all rotor efficiency shown. All the curves of this figure are terminated at a value of 50 percent of the compressor-exit total pressure, because, for lower values, atmospheric air could be supplied to the impeller inlet for the conditions of the analysis. That is, the compressor pressure ratio p_2'/p_1' is about 2.0 at an engine speed of 8000 rpm. Below the value of 50 percent of compressor-exit total pressure, further improvement in impeller performance would have no effect on either engine thrust or specific fuel consumption.

Points representing the experimentally determined percentage of compressor-exit total pressure required at the impeller inlet are also shown in figure 7(a). These points, which were obtained for the impeller without an inducer section when used with the turbine blade of figure 4(a) at an engine speed of 8000 rpm and coolant-flow ratios of 0.03 and 0.05, show that the impeller and blade combination operated with an efficiency of about 40 percent at a coolant-flow ratio of 0.03 and about -10 percent at a coolant-flow ratio of 0.05. This decrease in efficiency is primarily a result of the increase of blade pressure loss with increasing coolant flow, because the impeller pressure ratio does not vary significantly with coolant flow (fig. 8). The data points and the efficiency lines shown in figure 7(a) are for the specific impeller and blades of this report, but the curves of engine performance are general and cover a range of impellers that could be used in the hypothetical engines considered in the analysis.

The loss in engine thrust at a coolant-flow ratio of 0.03 is small for the impeller and blades of this report. No particular effort was made to obtain high aerodynamic performance for this impeller, and it appears that little consideration need be given to the aerodynamic performance when the impeller is operating at low cooling-air flows with blades having a pressure loss of about the same magnitude as these tube-filled blades. If the turbine blade cooling-air flow is expected to be high, or if the turbine blades have a high pressure loss, the performance of the impeller and blade combination may have a significant effect on the engine thrust and specific fuel consumption. This can be seen by observing the operating point of the straight impeller and blade

combination for a coolant-flow ratio of 0.05 in figure 7(a). The impeller requires about 73 percent of the compressor-exit total pressure for a coolant-flow ratio of 0.05 as compared with a compressor-exit total pressure of about 53 percent at a coolant-flow ratio of 0.03.

The variation of engine specific thrust and specific fuel consumption at the rated engine speed of 11,500 rpm is presented in figure 7(b). No efficiency lines or data points are included in this figure because of the lack of experimental information. At this engine speed, an increase in required total pressure at the impeller inlet from 50 to 100 percent of the compressor-exit total pressure results in a decrease in specific thrust from 56.9 to 56.3 pound-seconds per pound at the coolant-flow ratio of 0.03 (1.05 percent) and from 55.1 to 54.1 pound-seconds per pound at a coolant-flow ratio of 0.05 (1.81 percent). The corresponding increases in specific fuel consumption are from 1.256 to 1.272 lb/(hr)(lb) at a coolant-flow ratio of 0.03 (1.3 percent) and from 1.271 to 1.295 lb/(hr)(lb) at a coolant-flow ratio of 0.05 (1.9 percent). The decrease in actual engine thrust at a coolant-flow ratio of 0.03, if the required impeller-inlet total pressure varies from 50 to 100 percent of the compressor-exit total pressure, would be from 4310 to 4261 pounds (49-lb decrease), which is a small reduction in thrust. Therefore, it can be concluded that the loss in engine performance resulting from poor impeller performance will be relatively small at a coolant-flow ratio of 0.03, and even at a coolant-flow ratio of 0.05 the loss in engine thrust was only 74 pounds. If high coolant-flow ratios are anticipated (in excess of 0.05), the effect of impeller performance on engine performance at rated engine speed will probably have a greater significance than has been shown by the results of figure 7.

Impeller Total-Pressure Ratio

The performance of the impellers with and without inducer vanes is compared on the basis of the ratio of exit to entrance cooling-air total pressure in figure 8. The data for both impellers generally fall in the range of pressure ratio from about 0.97 to about 1.10. In order to give an idea of the relative impeller pressure ratio attainable ideally (100-percent-efficient impeller) for the diameter of the impellers considered here, the values of ideal impeller relative total-pressure ratio were calculated for impeller speeds of 4000, 6000, and 8000 rpm and are indicated in the figure. For example, at an engine speed of 8000 rpm the value of the impeller pressure ratio for either impeller could be increased to 1.22 by increasing the impeller efficiency to 100 percent. This is an increase of about 11 percent in impeller pressure ratio above the maximum experimental pressure ratio obtained. As will be pointed out later, attempts to approach this ultimate impeller performance by refining the impeller design will probably be unnecessary for air-cooled turbine blades that are now being considered for use in turbojet engines.

The calculation of the turbine blade pressure loss that was needed to obtain the impeller pressure ratio showed the necessity of determining the blade pressure loss accurately. To demonstrate this need, consider the impeller without inducer vanes and the blade used with it. At a coolant-flow ratio of 0.11 the total-pressure rise across the impeller is 0.74 inch of mercury and the total-pressure loss through the turbine blades is 22.6 inches of mercury. In view of the method used, it is obvious that a small inaccuracy in the calculation of the blade pressure loss will result in a large effect on impeller pressure ratio. The effect is not quite so serious at lower cooling-air flows where the blade pressure loss is smaller and therefore not such a large part of the over-all (impeller inlet to blade tip) pressure ratio.

The following three assumptions were made in calculating the blade pressure loss for the engine investigations that could affect the value of calculated blade pressure loss:

(1) No blockage of cooling-air flow area was caused by braze material.

(2) The local measured static pressure at the turbine blade tips (station 10) was the average static pressure at the blade tips.

(3) The cooling-air flow in the turbine blades is one-dimensional.

Because of these assumptions, the values of the pressure ratio across the cooling-air impeller may be somewhat in error, but, since the same procedures were used in the evaluation of the impeller pressure ratios of both rotors, the comparison between the performance of the two impellers was considered valid.

Cooling Air Available with Compressor Bleed

Turbine blade cooling with air bled from the compressor discharge is possible with the assumption of zero ducting loss only when the required total pressure at the cooling-air-impeller inlet is equal to or less than the total pressure available at the compressor discharge. The required total pressure at the impeller inlet is a function of the cooling-air weight flow, the impeller performance, and the pressure loss through the turbine blades. The operating range of the impellers of this report is compared with that of a hypothetical 100-percent-efficient impeller in figure 9 for an engine speed of 8000 rpm. The blade configuration of figure 4(a) was selected because it has a higher cooling-air pressure loss than that in figure 4(b), as is shown in appendix B. Use of blades with a relatively high pressure loss results in the most pessimistic evaluation of cooling-air-flow range. Because the impellers with or without inducer vanes have essentially the same performance (fig. 8), only a single line is shown in figure 9 for the operating range of both. The engine of this investigation using the blades of figure 4(a) can be

operated with air bled from the compressor exit over the part of the figure below the line of 100-percent compressor-exit total pressure and to the left of the impeller curves. Operation above the 100-percent line would require an auxiliary compressor to raise the cooling air to a pressure greater than the compressor-exit total pressure. The coolant-flow ratio corresponding to the point on the figure where the impeller operating line meets the line representing 100-percent compressor-exit total pressure is the limiting flow ratio for the particular impeller being considered. The two impellers of this report had a limiting coolant-flow ratio of 0.084; by increasing the efficiency to 100 percent, the limit of operation could be raised to a coolant-flow ratio of 0.103 with the particular tube-filled turbine blades used.

Tube-filled turbine blades made of nonstrategic alloy Timken 17-22A(S) similar to the turbine blades considered in this figure may operate safely at 11,500 rpm (rated engine speed) with a combustion-gas temperature of 1450° F, a cooling-air temperature of 450° F, and a coolant-flow ratio of about 0.025 (ref. 11). Therefore, when either the impeller with or the one without inducer vanes is used with turbine blades such as these, the maximum supply of cooling air available is about three times greater than the required quantity of cooling air for adequate cooling of the turbine blades. The limits that are presented are not absolute limits for the operation of the cooling-air impellers considered here. These limits would become lower if a blade having a higher pressure loss were considered and would become higher for a blade of lower pressure loss.

General Comments

The analytical results show that turbojet-engine performance is not extremely sensitive to the turbine cooling-air-impeller performance at rated engine speed for coolant-flow ratios up to 0.05; however, its significance should be evaluated on the basis of the type of aircraft in which the engine will be used. The experimental results indicate that the performance of the impellers with and without an inducer section is essentially the same and that either impeller would supply about three times as much cooling air as is necessary to cool turbine blades made of noncritical material at present-day turbine-inlet temperatures. Because impellers with and without inducer sections have about the same performance and because the effect of impeller performance on engine performance is not great, it appears that impellers having no inducer sections can be used on cooled turbojet engines designed for current or somewhat higher turbine-inlet temperatures without adversely affecting engine or cooling performance. Furthermore, it is easier to fabricate rotors with straight radial vanes (no inducer section) than rotors with an inducer. For future high-temperature engines, where blades having high pressure losses, or requiring large amounts of cooling air, or both, may be employed, relatively slight differences in impeller

pressure ratio may affect the cooling performance of the blades to such a degree that design refinements of the cooling-air impellers may be required.

SUMMARY OF RESULTS

The results of an analytical and experimental investigation of turbine cooling-air impellers are summarized as follows:

1. The results of an analytical investigation to determine the effect of impeller performance on engine performance showed that, at rated engine speed (11,500 rpm) and a coolant-flow ratio of 0.03, the effects of impeller performance on engine performance were small. For example, increasing the required impeller-inlet total pressure from 50 to 100 percent of the compressor-exit total pressure decreased engine thrust about 1 percent and increased specific fuel consumption 1.3 percent. When the coolant-flow ratio was increased to 0.05, the decrease in thrust and increase in specific fuel consumption were 1.8 and 1.9 percent, respectively.

2. The experimental data obtained from impellers with and without inducer sections indicated that the relative total-pressure ratios for both impellers were about the same. They ranged from about 0.97 to 1.10 for engine speeds of 4000, 6000, and 8000 rpm. Either cooling-air impeller could supply the same quantity of cooling air to a given set of turbine blades, because the relative total-pressure ratios of the two impellers investigated were essentially the same. If the cooling-air impellers used tube-filled turbine blades having a relatively high pressure loss and were operated in an engine at 8000 rpm, either would be capable of supplying cooling air at a rate equivalent to a coolant-flow ratio of about 0.084 (about three times the quantity of coolant required to cool turbine blades made of nonstrategic material at present-day turbine-inlet temperatures). Turbine cooling-air impellers without inducer sections, which are easier to fabricate than impellers with inducer sections, appear to offer satisfactory performance for use with nonstrategic turbine blades at current gas temperatures or with strategic turbine blades at higher gas temperatures.

Lewis Flight Propulsion Laboratory
    National Advisory Committee for Aeronautics
        Cleveland, Ohio, August 16, 1954

APPENDIX A

SYMBOLS

The following symbols are used in this report:

A cross-sectional area, sq ft

c_p specific heat at constant pressure, Btu/(lb)($^{\circ}$R)

D_h hydraulic diameter, $\dfrac{4 \text{ times flow area}}{\text{wetted perimeter}}$, ft

F thrust, lb

Fr friction due to contraction, ft-lb/lb

f fuel-air ratio

fr_K friction factor as determined from von Kármán equation,
$1/\sqrt{fr_K} = 4.0 \log (Re\sqrt{fr_K}) - 0.40$

g acceleration due to gravity, ft/sec^2 or lb mass/slugs

h convection heat-transfer coefficient, Btu/(sec)(sq ft)($^{\circ}$R)

h_f effective inside heat-transfer coefficient, Btu/(sec)(sq ft)($^{\circ}$R)

J mechanical equivalent of heat, 778.2 ft-lb/Btu

K pressure-loss coefficient

k thermal conductivity, Btu/(sec)(ft)($^{\circ}$R)

L effective fin length, ft

M Mach number

m fin spacing, ft

N nominal engine speed, rpm

p static pressure, lb/sq ft or in. Hg abs

p' total pressure, lb/sq ft or in. Hg abs

R gas constant, ft-lb/(lb)($^{\circ}$R)

Re   Reynolds number

r   radius, ft

S   blade-shell inside-surface area, sq ft

T   static temperature, $^{\circ}$R

T'   total temperature, $^{\circ}$R

V   velocity, ft/sec

w   weight-flow rate, lb/sec

γ ratio of specific heats

δ ratio of absolute total pressure at given station to absolute
      total pressure at NACA standard sea-level conditions, p'/2116

η efficiency

θ ratio of absolute total temperature at given station to absolute
      total temperature at NACA standard sea-level conditions,
      T'/518.7° R

μ absolute viscosity, slugs/(sec)(ft)

ρ density, lb/cu ft

τ fin thickness, ft

φ $\sqrt{2\overline{h}_{a,b}/\overline{\tau}k_b}$

$\mathfrak{L}_a$ power expended on cooling air within turbine rotor, Btu/sec

$\mathfrak{L}_C$ compressor power, Btu/sec

$\mathfrak{L}_T$ turbine power, Btu/sec

ω angular velocity, radians/sec

Subscripts:

a   cooling air

b   blade (refers to quantities based on blade temperature when used
      with Re, μ, and k)

C   compressor

c   contraction

F   fuel

film   refers to quantities based on film temperature between
                cooling air and blade shell

H   heat transfer

R   rotation

T   turbine

1,2,3,4,5   stations through engine (see figs. 5 and 6)
6,7,8,9,10

Superscripts:

'   total conditions

"   total conditions relative to turbine rotor

—   average value

APPENDIX B

BLADE PRESSURE-LOSS CALIBRATION

As has been pointed out in the body of the report, the blade and blade-base cooling-air pressure loss must be calculated so that the impeller pressure ratios can be evaluated from the engine data. The pressure loss through the cooling-air passages of the blade is calculated with the charts of reference 7, and the pressure loss across the blade base is evaluated from the equation

$$\Delta p'_{7-8} = K \left(\frac{\rho V^2}{2g} \right)$$

Before these calculations were made with the engine data, mock-ups of a sector of the turbine disk of reference 3 and of this report were fabricated. The proper turbine blade was mounted on each sector. These mock-ups were made to permit the experimental evaluation of the base pressure-loss coefficient for the blade of this report and the blade of reference 3 and also to check whether friction factors known to be applicable to circular pipes could be used with the reference 7 pressure-loss charts to calculate the friction pressure loss through the blade cooling-air passages of the two blades. A check of the use of pipe friction factors with tube-filled turbine blades was also made in reference 12, which stated that pipe friction factors as defined by the von Kármán equation permit the calculation of the blade pressure loss with an accuracy of 6 percent. The repeat of the check of the use of pipe friction factors for calculating the friction pressure loss through a tube-filled turbine blade was made in this report because the blade cooling-air-flow passages were partially blocked with braze material and also the blades of this investigation had bases fastened to the blade shells that gave a cooling-air entrance to the blades that was different from that in reference 12.

Blade Pressure-Loss Calibration Rig and Instrumentation

The blade pressure-loss calibration rig consisted of a mock-up section of one cooling-air passage within each of the cooling-air impellers. The mock-up rotor section without an inducer is shown disassembled in figure 10(a) and for the rotor with an inducer section in figure 10(b). An assembled view of the mock-up sector for the rotor with the inducer vanes is shown in figure 11. The assembled mock-up sector for the rotor without inducer vanes had essentially the same exterior appearance.

The mock-up rotor segments were made of brass and each contained a full-scale duplication of one cooling-air-flow passage.

The location of instrumentation in the mock-up rotor segments is shown in figure 12. Four static-pressure measurements were made at the exit of the impeller passage (entrance to the blade base) in a plane 5.1 inches from the blade tip in each mock-up; the pressures were measured at a point midway along each of the four walls of the impeller cooling-air passage. Total-pressure surveys were made at the tip of both blades and at a plane about 0.1 inch inside the entrance to the cooling-air passages. For the blades used in the rotor without an inducer section, this plane was 4.4 inches from the blade tip; and for the blades used in the rotor with the inducer section, the plane was 3.9 inches from the blade tip. These total-pressure measurements were made in each of the blade cooling-air passages with a movable probe that was inserted from the blade tip. This probe was made from stainless steel tubing having an outside diameter of 0.020 inch.

Air was supplied to the test sections at room temperature from a laboratory high-pressure air system. The air was exhausted from the blade tips into the test cell, which was at barometric pressure. The air flow was controlled with hand-operated valves and was measured with calibrated air rotameters about 10 feet upstream of the test sections. Air temperature was measured by an iron-constantan thermocouple installed at the inlet to the rotameters.

Experimental Procedure

The measuring and calculating station numbers are shown in figure 12.

The total-pressure drop across the blade base and across the blade cooling-air passage was determined for a range of air weight flows from 0.016 to 0.08 pounds per second in eight increments. At each weight flow a total-pressure survey was made at stations 8 and 9. These surveys consisted of a total-pressure measurement in each of the cooling-air passages in the blade at both of these stations. The probe was positioned in each passage to give a maximum reading. The four static pressures at the entrance to the blade base (station 7) were also recorded for each weight flow and were used to calculate the total pressure at this station. The probe readings could be repeated within about 0.1 inch of mercury or about 2 percent.

The total air temperature and the air weight-flow rate were also measured for each survey.

The same procedure was followed for both mock-ups of the disk and blade combinations.

Calculation Procedure

A comparison between the calculated and the measured total-pressure loss through the cooling-air passage of the turbine blades on the mock-up

was made to check the applicability of the pipe friction factors and the charts of reference 7 for calculating the total-pressure loss through the turbine blades due to friction. The pressure-loss evaluation is made starting with the cooling-air Mach number at the blade tip and working through the blade to obtain the Mach number at the inlet to the cooling-air passage. One-dimensional adiabatic flow conditions are assumed in these calculations. The following two parameters must be evaluated in order to use the pressure-loss charts of reference 7:

Tip Mach number M_9

Friction parameter $\dfrac{4fr_K(r_9 - r_8)}{D_h}$

The cooling-air Mach number at the blade tip is calculated with the energy equation and the continuity equation, which are combined to give

$$\frac{w_a\sqrt{T'}}{pA_9} = \sqrt{\frac{\gamma g}{R}}\, M_9 \sqrt{\left(1 + \frac{\gamma - 1}{2} M_9^2\right)} \tag{B1}$$

The cooling-air passage flow area used in this calculation for the pressure-loss calibration tests was the actual cooling-air-flow area of the blade mounted on the disk mock-up. This area was measured at the blade tip.

The friction factor needed in the evaluation of the friction parameter is obtained from von Kármán friction-factor equation, which can be written as

$$1/fr_K = 4.0 \log \left(Re \sqrt{fr_K}\right) - 0.40 \tag{B2}$$

which gives the friction factor for established turbulent flow. Reference 13 states that a passage length at least equal to $40(L/D_h)$ is required to obtain established turbulent flow. This requirement means that most of the blade span will be needed to obtain established flow, since the diameter of the cooling-air tubes was 0.10 inch. Thus, the friction factor as obtained from equation (B2) is increased by 5 percent to account for the entrance effect, according to reference 14, before it is used to evaluate the friction parameter. Hereafter, this friction factor will be called corrected friction factor. The Reynolds number needed in equation (B2) is evaluated from the equation

$$Re = w_a D_h / A_9 \mu g \tag{B3}$$

The value of the Mach number at station 8 is then obtained from the pressure-loss charts with the friction parameter and the Mach number at station 9. The total cooling-air pressure at station 8 is calculated from the values of the Mach number, the total cooling-air temperature,

the cooling-air weight flow, and the cooling-air-flow passage area at station 8 with the continuity equation. This procedure is used to determine the friction pressure loss through the blade cooling-air passage.

The pressure loss through the blade base is essentially a sudden contraction loss. According to reference 15, this type of loss can be expressed as

$$Fr = K\left(\frac{V^2}{2g}\right) \tag{B4}$$

where Fr is the friction due to sudden contraction (ft-lb/lb of fluid). The total-pressure loss due to sudden contraction can be written as

$$\Delta p'_c = K\left(\frac{\rho V^2}{2g}\right) \tag{B5}$$

In order to use equation (B5) to evaluate the base loss coefficient for both blade base configurations, it is written in the form

$$\frac{p'_7 - p'_8}{p_8} = K\left(\frac{w_a^2 T_8}{A_8^2 p_8^2}\right)\frac{R}{2g} \tag{B6}$$

The total pressure p'_7 is calculated from the measured values of p_7, w_a, T'_a, and A_7. The total pressure at station 8 is obtained from the surveys made at this station. The static pressure at station 8 is calculated from the measured values of p'_8, w_a, T'_a, and A_8. The total air temperature is used in place of the static temperature at station 8, inasmuch as the Mach number at this station is low. This base pressure-loss coefficient then permits the calculation of the pressure drop across the blade base from stations 7 to 8, which can be added to the pressure loss from stations 8 to 9 to give the over-all pressure drop across the turbine blade and blade base. The identical procedure was used in calculating the pressure drop across both blade configurations; however, individual blade base pressure-loss coefficients were determined experimentally for each of the blades.

Results of Pressure-Loss Calibration

The base loss coefficients for both blades are calculated with equation (B6). The base loss coefficients obtained for the range of air flows investigated were averaged arithmetically. The average coefficient obtained for the base of the blade used on the impeller with no inducer vanes was 0.62 and that for the blade used on the impeller with inducer vanes was 0.23.

The pressure loss resulting from a sudden contraction is a function of the ratio of the two flow areas involved. Values of contraction loss coefficients for a range of area ratios are presented in reference 15. The calculated contraction loss coefficients (stations 7 to 8) obtained from reference 15 for both blades are 0.38 for the blade used with the impeller without inducer vanes and 0.26 for the blade used with the impeller with inducer vanes. The value of 0.38 does not agree well with the experimental value of 0.64, but the value of 0.26 for the other blade agrees very well with the experimental value of 0.23. These values cannot be expected to agree exactly with the experimental values of base loss coefficients, because the flow into the blade base is probably not established turbulent flow and the contraction is not from a single large passage into a single small passage, but rather from a single large passage into several small irregular-shaped cooling-air passages in the turbine blade. In spite of this possible inaccuracy, the procedure for obtaining a calculated blade base loss coefficient would probably be satisfactory for a design study, because the blade base pressure loss for the type of blades used here is about 20 percent of the over-all pressure loss across the blade, and, therefore, an error in the base pressure loss will have only a minor effect on the over-all blade pressure loss.

A comparison of the total cooling-air pressure loss from stations 7 to 9 of both of the turbine blades investigated in the calibration rig is presented in figure 13. The data show that the pressure loss across the blade used in the rotor without inducer vanes was about twice the pressure loss of the blade used in the rotor with inducer vanes. For the blade used with the rotor without inducer vanes, about 80 percent of the total-pressure loss occurred in the blade cooling passage and 20 percent in the blade base. For the blade used on the rotor with inducer vanes, 90 percent of the total-pressure loss occurred in the blade and 10 percent in the blade base.

The accuracy with which the friction pressure loss through the turbine blade can be calculated by using the corrected pipe friction factors and the charts of reference 7 is demonstrated by comparing the calculated total pressure at station 7 with the value obtained experimentally for this station. The calculated total pressure at station 7 was obtained by adding the calculated total-pressure loss through the turbine blade to the total pressure at the blade tip. This comparison (fig. 14) indicates that the use of pipe friction factors with the charts of reference 7 permits sufficiently accurate calculation of the pressure loss through the turbine blades that were used in this investigation. The maximum error in the calculation of the total pressure at station 7 was 3.0 inches of mercury or 8.7 percent. The comparison demonstrates that, for the condition of zero heat transfer to the cooling air and zero rotation, the accuracy of the calculation of the pressure loss through the turbine blade is good. In reference 12 the effect of heat transfer on the accuracy of turbine blade pressure-loss calculations was evaluated and it was concluded that even in the presence of heat transfer the cooling-air pressure

loss through tube-filled blades could be calculated with a reasonable
degree of accuracy when the friction factor was evaluated for the condi-
tion of zero heat transfer. Since there were no instruments available
for measuring pressures on a rotating turbine, no check of the accuracy
of the calculation of the total-pressure change through the turbine blade
due to rotation could be made.

<div align="center">REFERENCES</div>

1. Schey, Oscar W.: The Advantages of High Inlet Temperature for Gas
     Turbines and Effectiveness of Various Methods of Cooling the Blades.
     Paper No. 48-A-105, presented at A.S.M.E. meeting (New York), Nov.
     28-Dec. 3, 1948.

2. Hubbartt, James E., Rossback, Richard J., and Schramm, Wilson B.:
     Analysis of Factors Affecting Selection and Design of Air-Cooled
     Single-Stage Turbines for Turbojet Engines. III - Engine Design-
     Point Performance. NACA RM E54F16a, 1954.

3. Nachtigall, Alfred J., Zalabak, Charles F., and Ziemer, Robert R.:
     Investigations of Air-Cooled Turbine Rotors for Turbojet Engines.
     III - Experimental Cooling-Air Impeller Performance and Turbine
     Rotor Temperatures in Modified J33 Split-Disk Rotor up to Speeds
     of 10,000 RPM. NACA RM E52C12, 1952.

4. Kemp, Richard H., and Moseson, Merland L.: Investigations of Air-
     Cooled Turbine Rotors for Turbojet Engines. II - Mechanical Design,
     Stress Analysis, and Burst Test of Modified J33 Split-Disk Rotor.
     NACA RM E51J03, 1952.

5. Schramm, Wilson B., and Ziemer, Robert R.: Investigations of Air-
     Cooled Turbine Rotors for Turbojet Engines. I - Experimental Disk
     Temperature Distribution in Modified J33 Split-Disk Rotor at Speeds
     up to 6000 RPM. NACA RM E51I11, 1952.

6. Long, Roger A., and Esgar, Jack B.: Experimental Investigation of
     Air-Cooled Turbine Blades in a Turbojet Engine. VII - Rotor-Blade
     Fabrication Procedures. NACA RM E51E23, 1951.

7. Hubbartt, James E., Slone, Henry O., and Arne, Vernon L.: Method for
     Rapid Determination of the Pressure Change for One-Dimensional Flow
     with Heat Transfer, Friction, Rotation, and Area Change. NACA TN
     3150, 1954.

8. Livingood, John N. B., and Brown, W. Byron: Analysis of Spanwise
     Temperature Distribution in Three Types of Air-Cooled Turbine
     Blades. NACA Rep. 994, 1950. (Supersedes NACA RM's E7B11e and
     E7G30.)

9. Ziemer, Robert R., and Slone, Henry O.: Analytical Procedures for
     Rapid Selection of Coolant Passage Configurations for Air-Cooled
     Turbine Rotor Blades and for Evaluation of Heat-Transfer, Strength,
     and Pressure-Loss Characteristics. NACA RM E52G18, 1952.

10. Humble, Leroy V., Lowdermilk, Warren H., and Desmon, Leland G.:
     Measurements of Average Heat-Transfer and Friction Coefficients
     for Subsonic Flow of Air in Smooth Tubes at High Surface and Fluid
     Temperatures. NACA Rep. 1020, 1951. (Supersedes NACA RM's E7L31,
     E8L03, E50E23, and E50H23.)

11. Esgar, Jack B., and Clure, John L.: Experimental Investigation of
     Air-Cooled Turbine Blades in Turbojet Engine. X - Endurance
     Evaluation of Several Tube-Filled Rotor Blades. NACA RM E52B13,
     1952.

12. Brown, W. Byron, and Slone, Henry O.: Pressure Drop in Coolant
     Passages of Two Air-Cooled Turbine-Blade Configurations. NACA
     RM E52D01, 1952.

13. Eckert, E. R. G.: Introduction to the Transfer of Heat and Mass.
     McGraw-Hill Book Co., Inc., 1950.

14. Shapiro, Ascher H., and Smith, R. Douglas: Friction Coefficients in
     the Inlet Length of Smooth Round Tubes. NACA TN 1785, 1948.

15. McAdams, William M.: Heat Transmission. Second ed., McGraw-Hill
     Book Co., Inc., 1942.
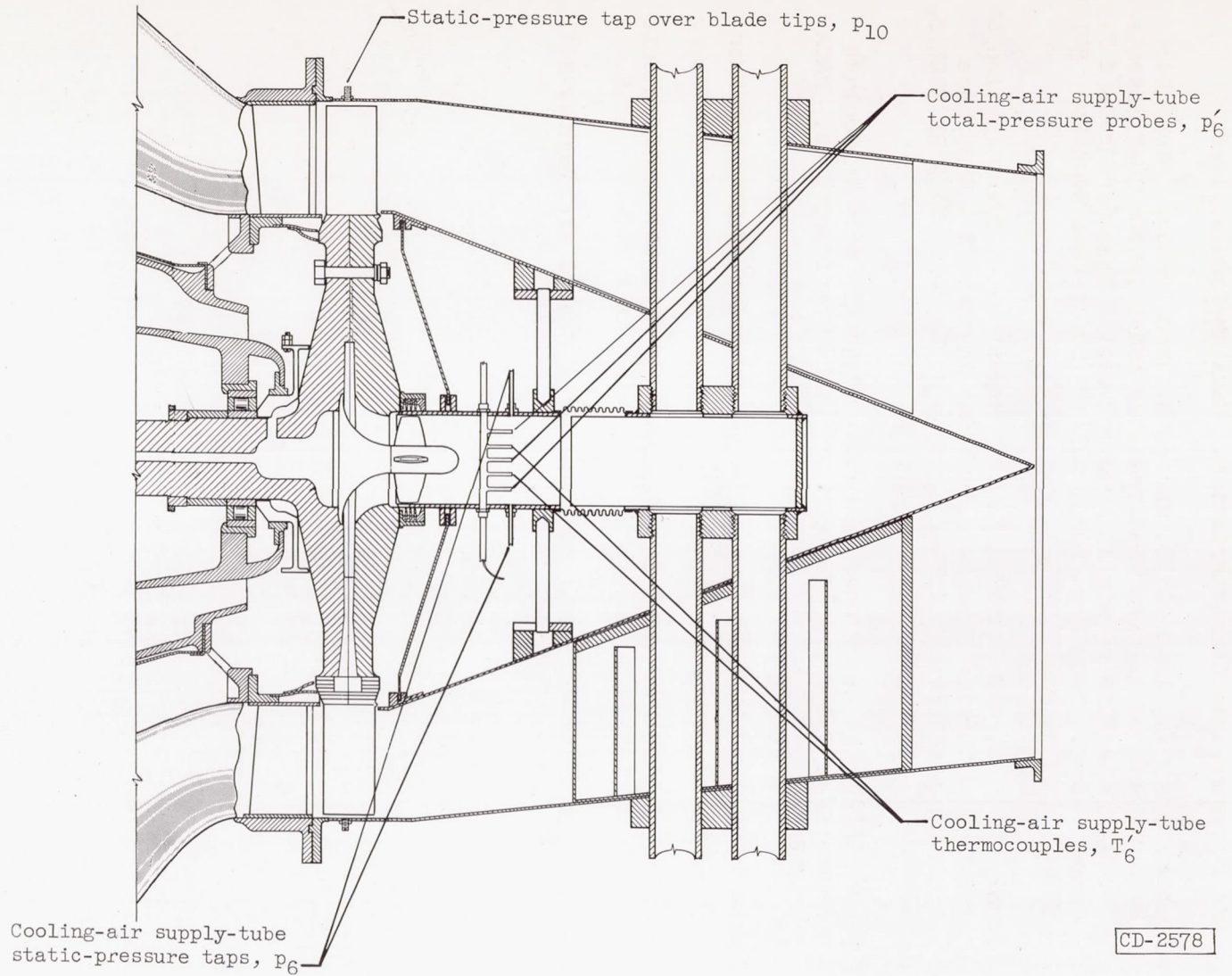
Figure 1. - Engine modifications and cooling-air instrumentation.

Static-pressure tap over blade tips, p_{10}

Cooling-air supply-tube total-pressure probes, p_6'

Cooling-air supply-tube thermocouples, T_6'

Cooling-air supply-tube static-pressure taps, p_6

CD-2578

(a) Rotor without inducer.

C-36598
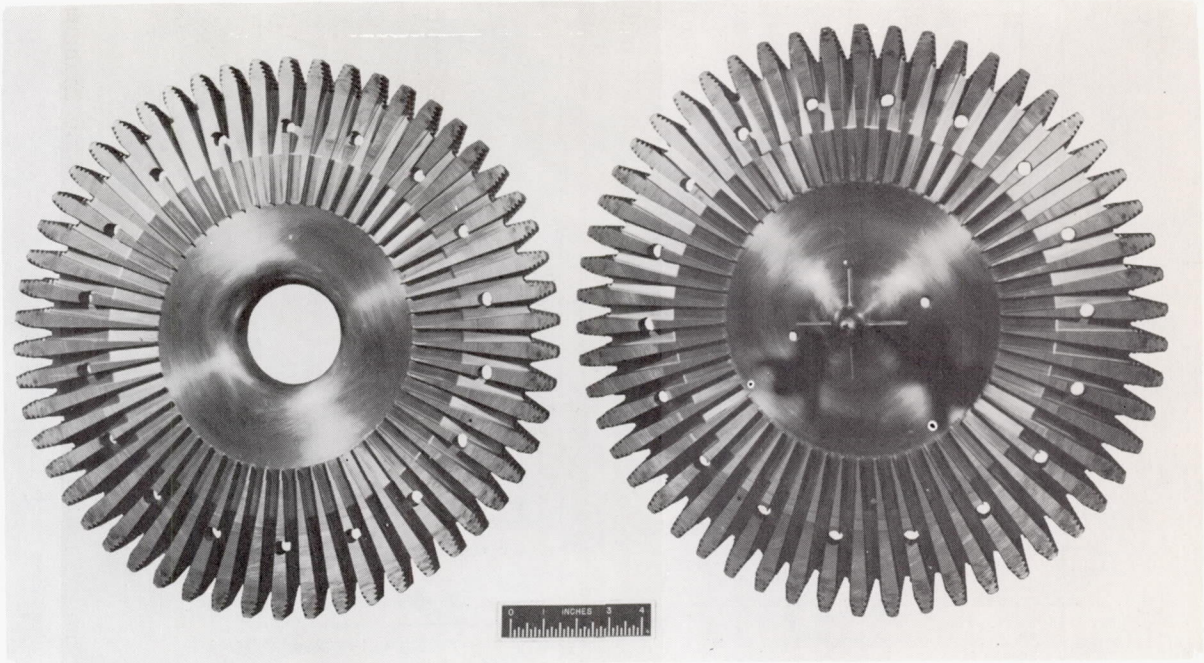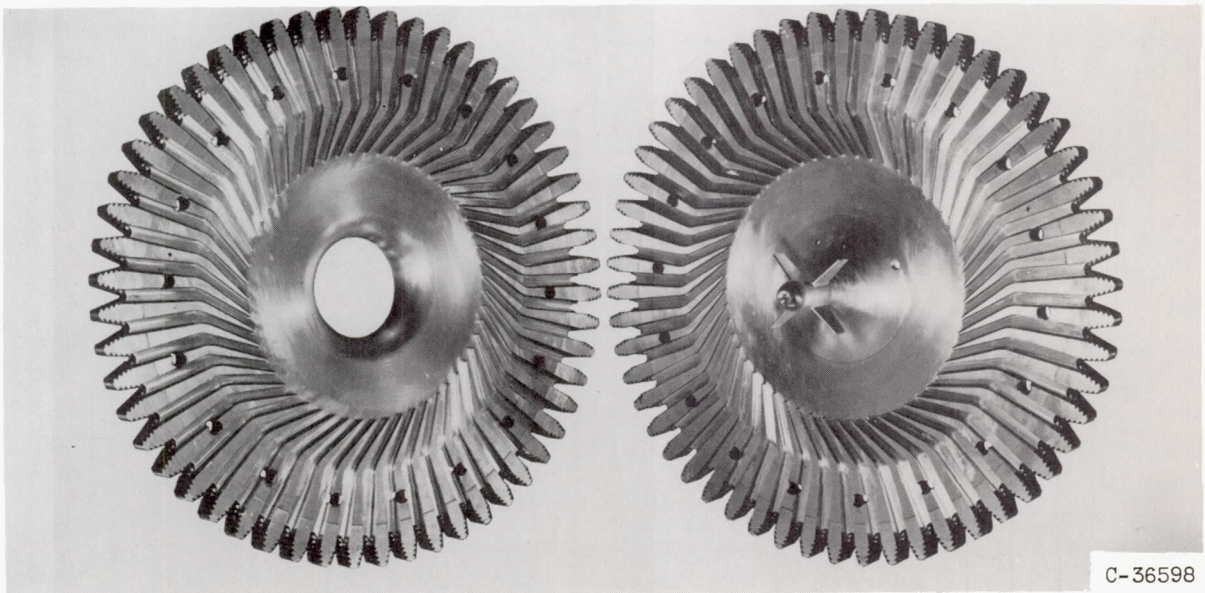
Rear half of rotor   Front half of rotor

(b) Rotor with inducer vanes (refs. 3 and 4).

Figure 2. - Split-disk cooling-air impellers with and without inducer vanes at impeller inlet.

Figure 3. - Comparison of geometry of air-cooled rotor without inducer section and rotor with inducer section. (All dimensions in inches or degrees.)

Length of cooling air tubes

C-36512
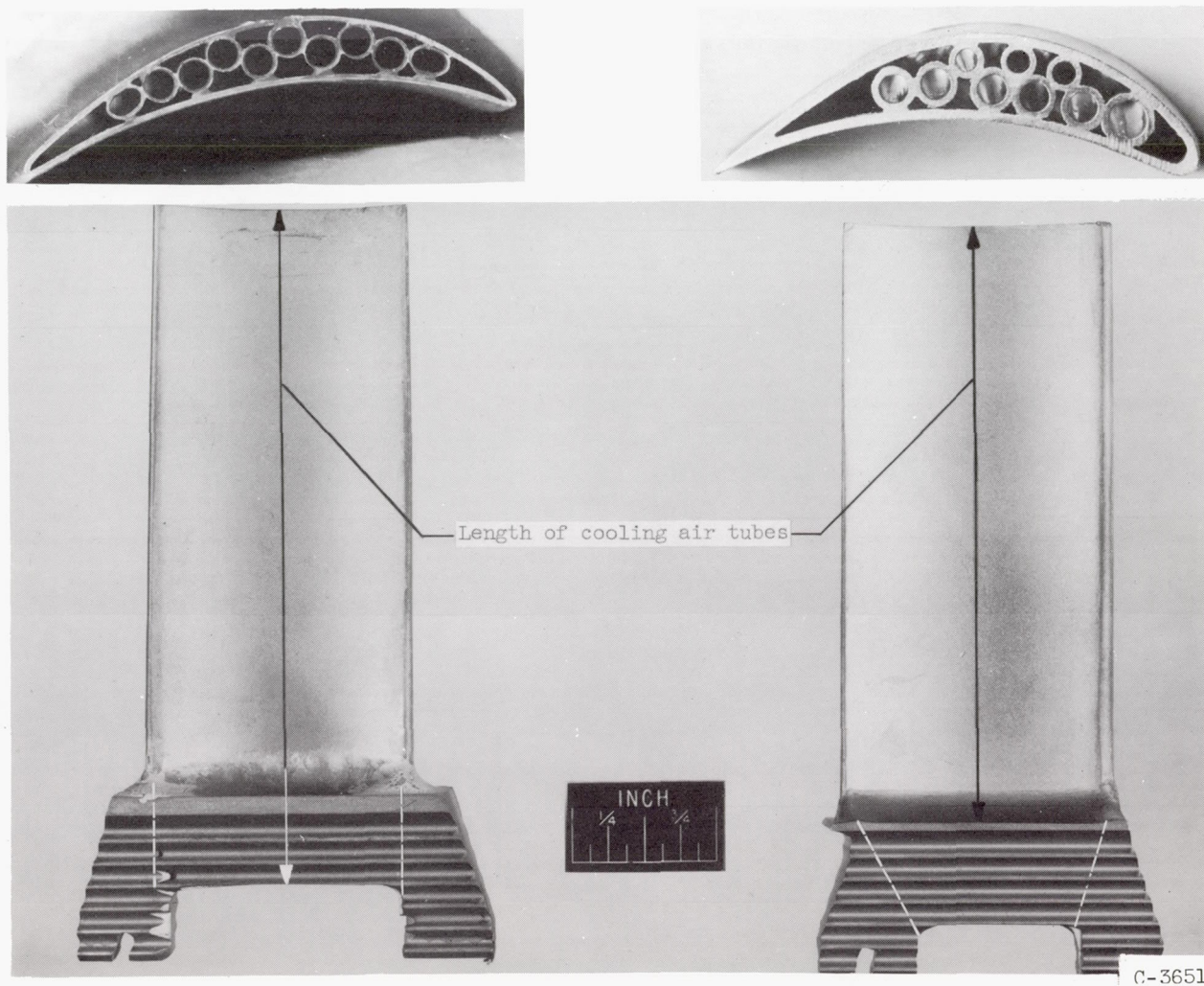
(a) Blade used in impeller
without inducer vanes.

(b) Blade used in impeller with
inducer vanes (ref. 3).

Figure 4. - Air-cooled turbine blades used in impeller investigations.
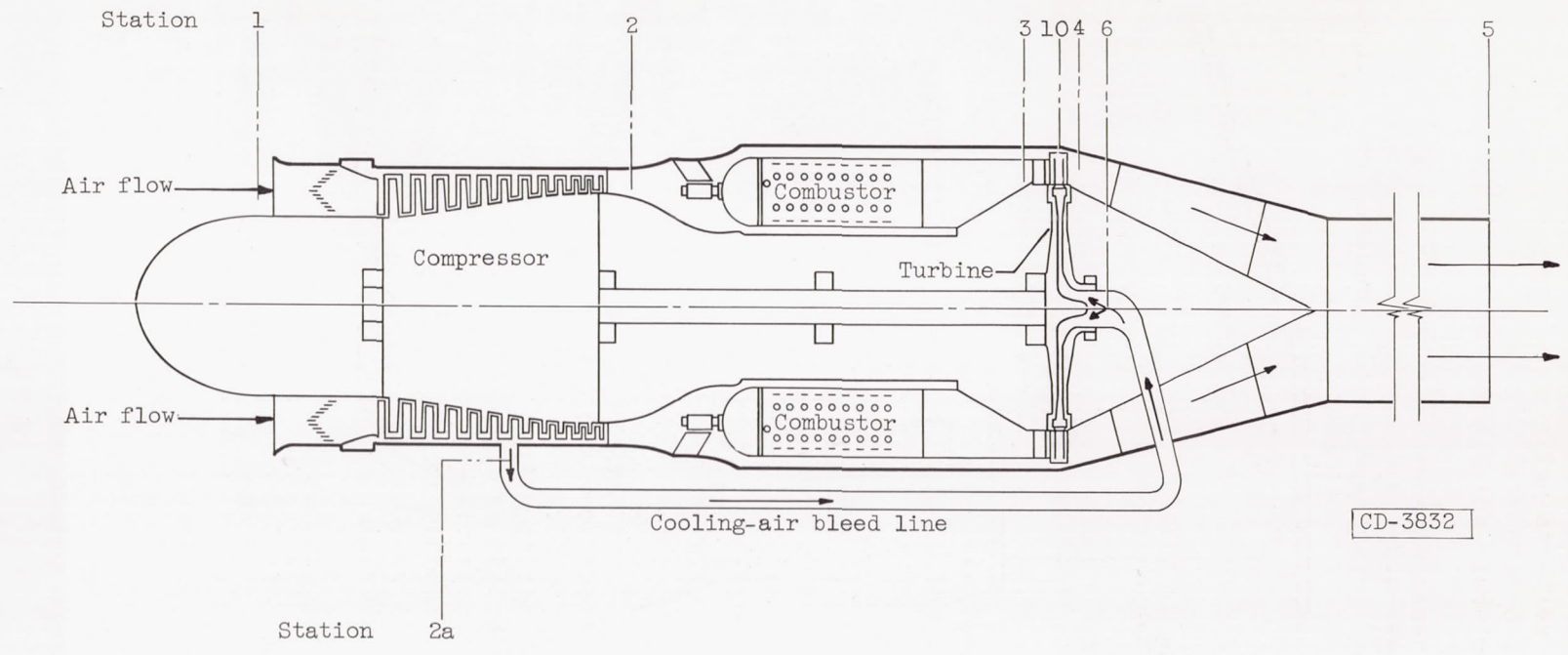
Figure 5. - Stations for engine performance calculations.
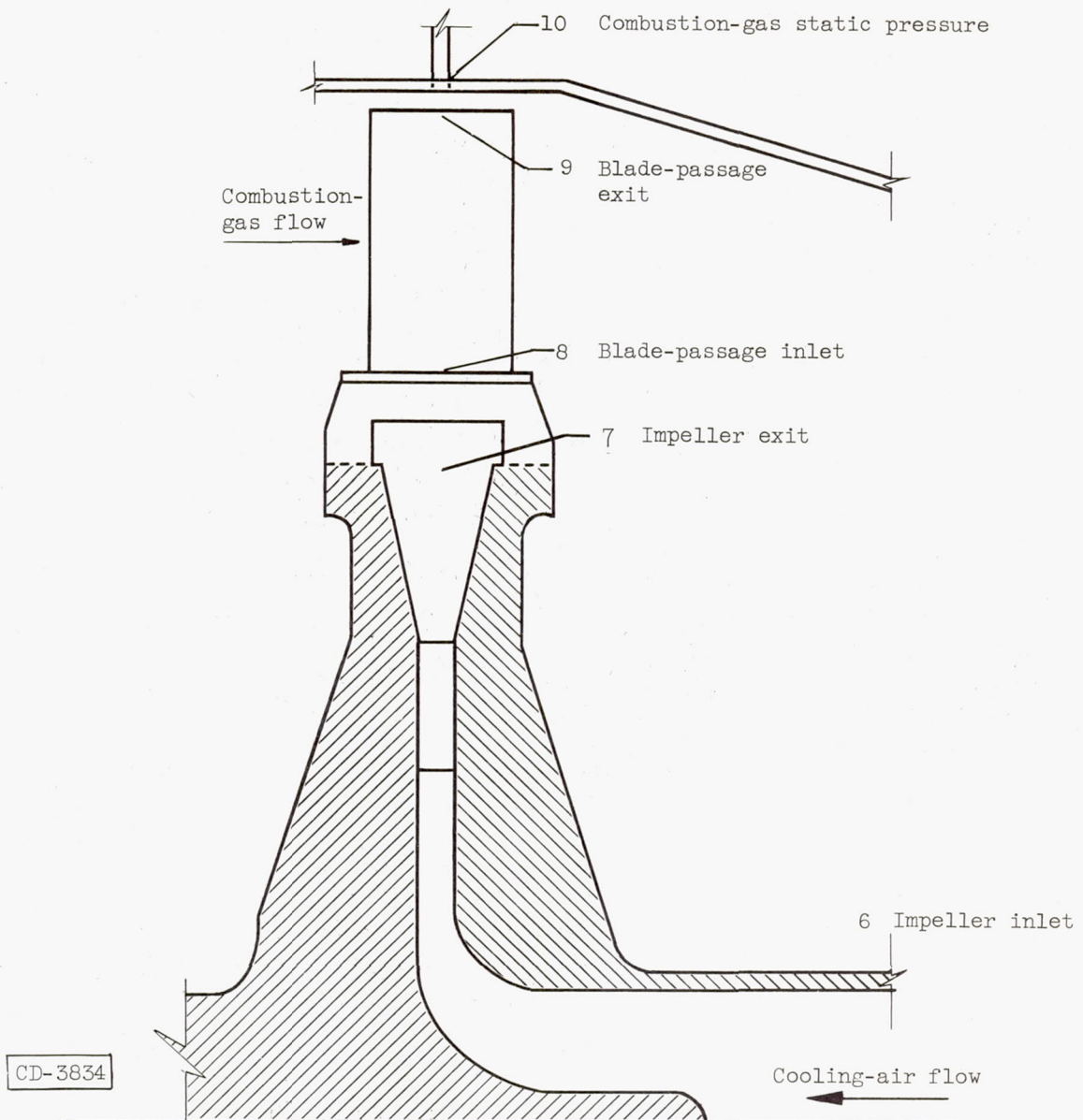
Figure 6. - Impeller measuring and calculating stations.
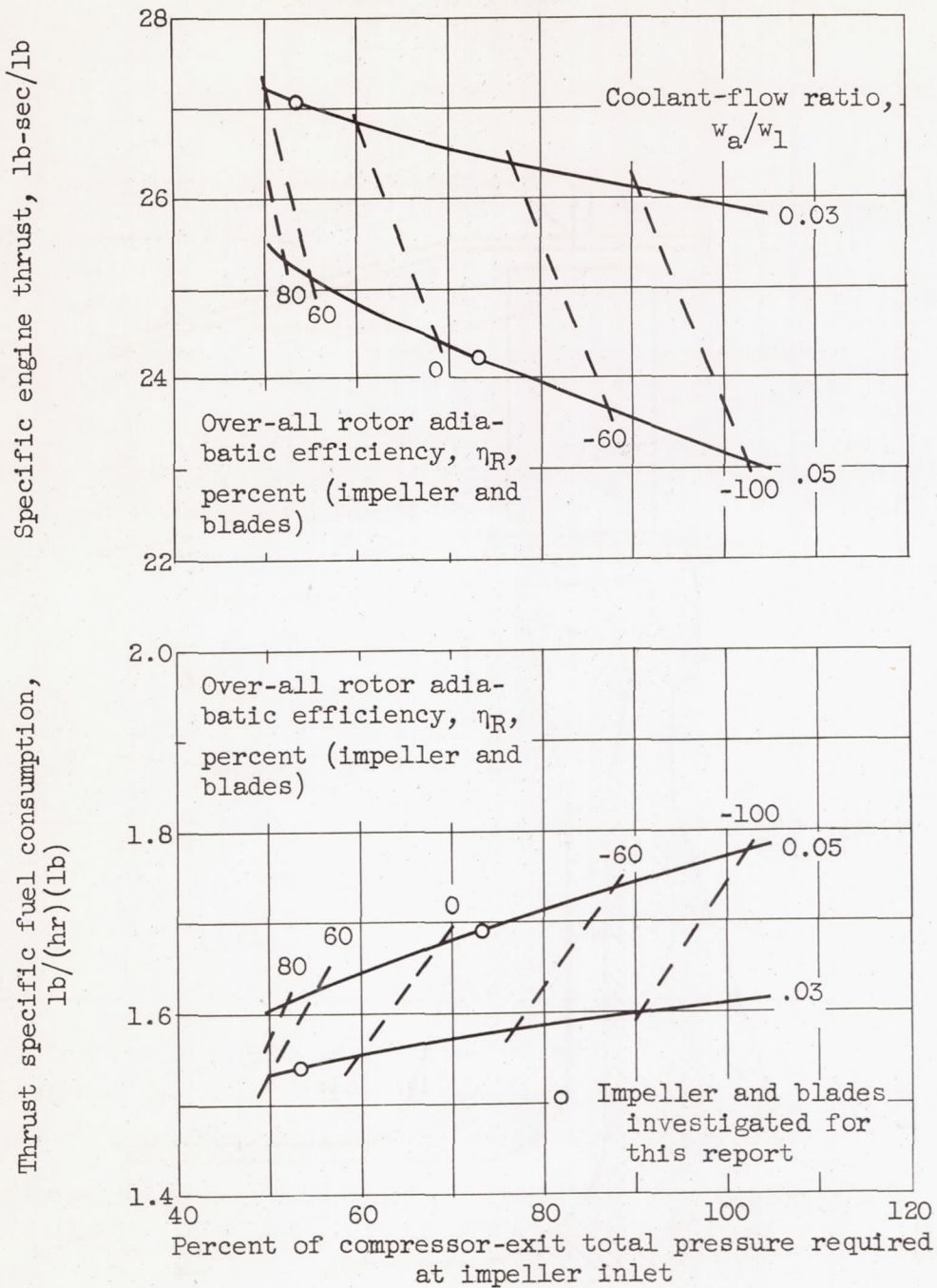
(a) Engine speed, 8000 rpm.

Figure 7. - Variation of specific thrust and specific
fuel consumption with cooling-air-impeller perform-
ance.
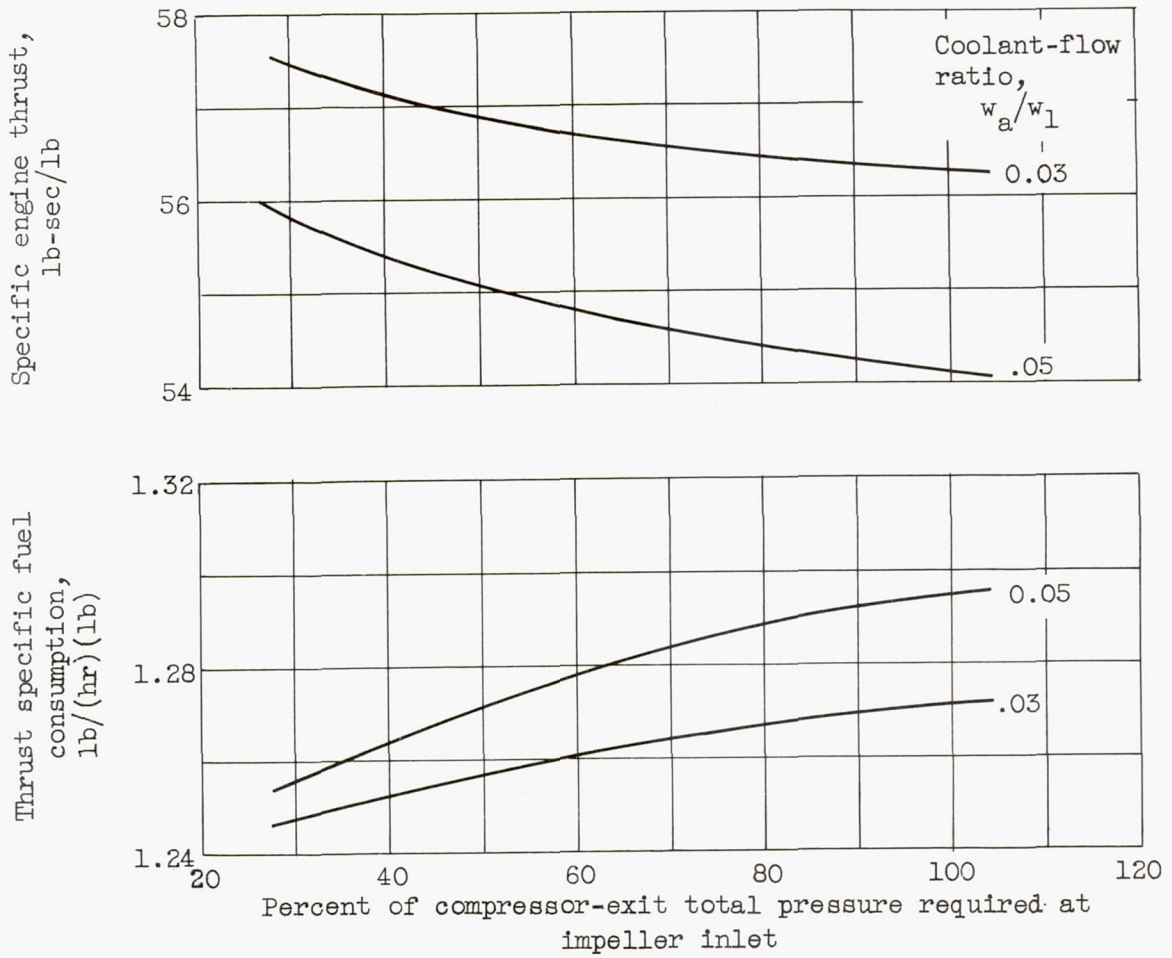
(b) Engine speed, 11,500 rpm.

Figure 7. - Concluded. Variation of specific thrust and
specific fuel consumption with cooling-air-impeller
performance.
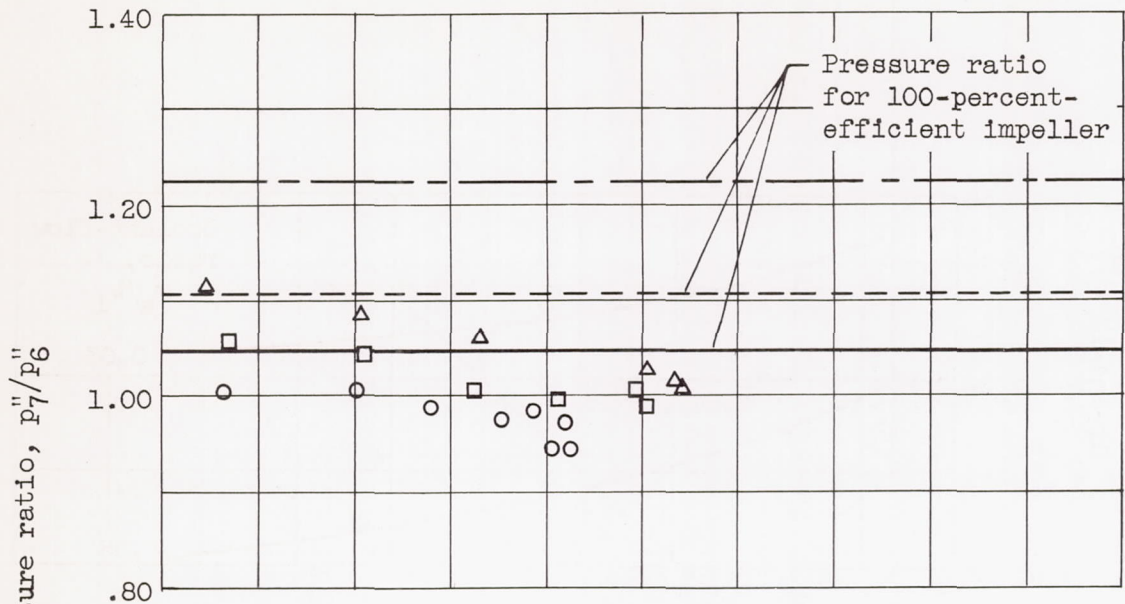
(a) Impeller without inducer vanes.
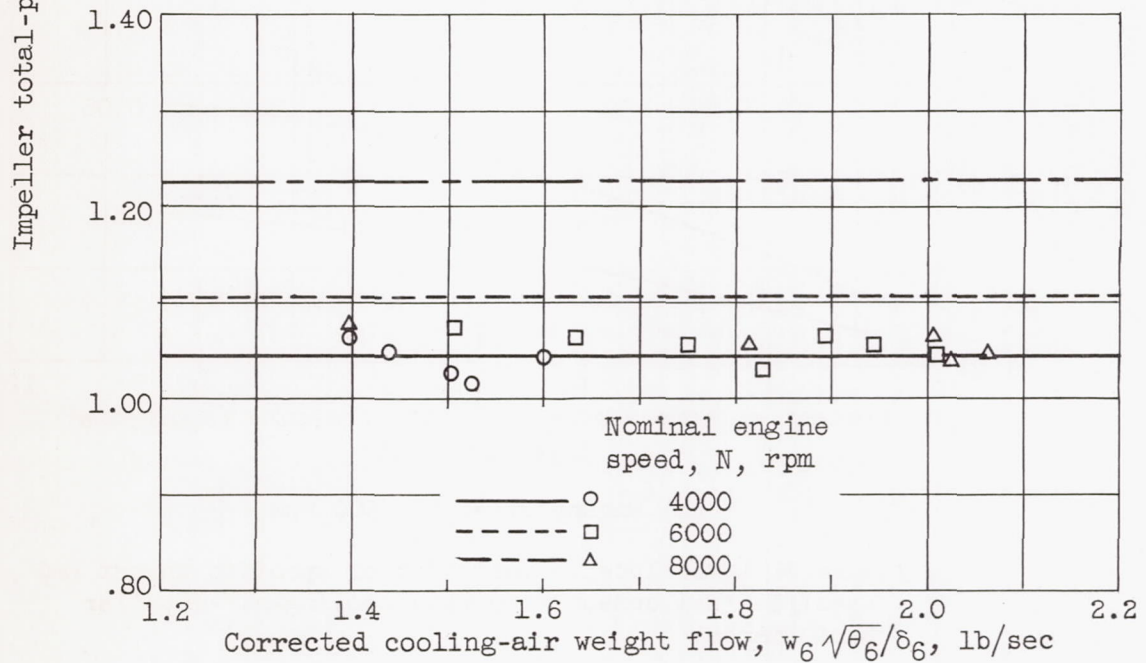
(b) Impeller with inducer vanes.

Figure 8. - Variation of impeller pressure ratio with cooling-air flow and impeller speed.
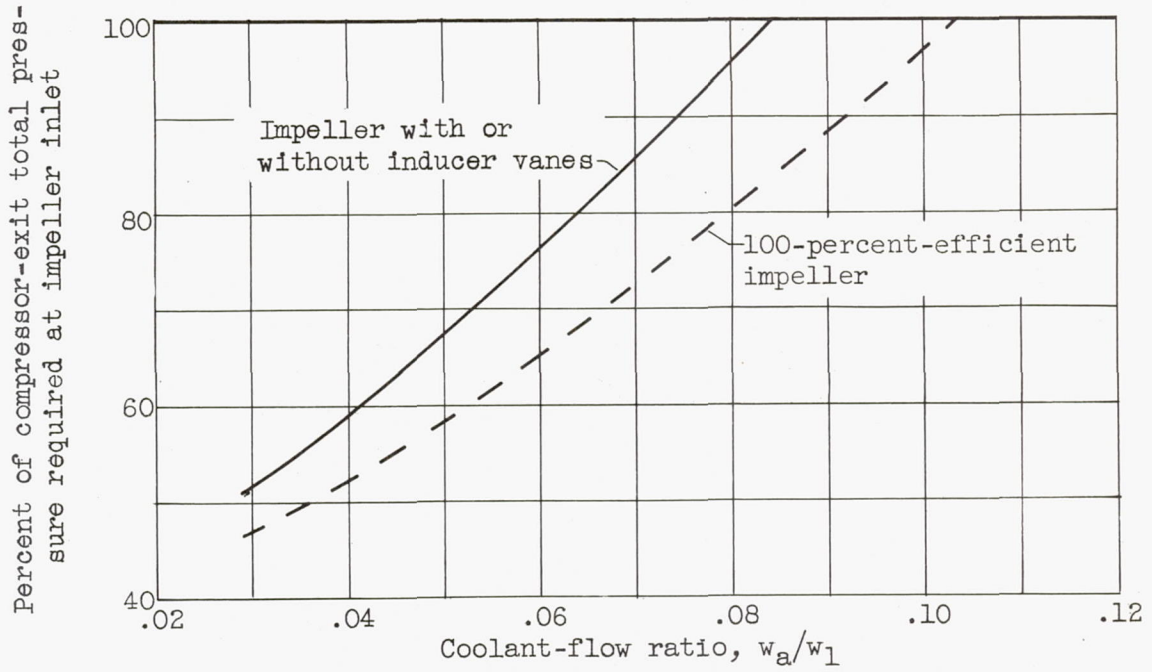
Figure 9. - Range of cooling-air-impeller operation when
cooling air is bled from compressor. Engine speed,
8000 rpm.
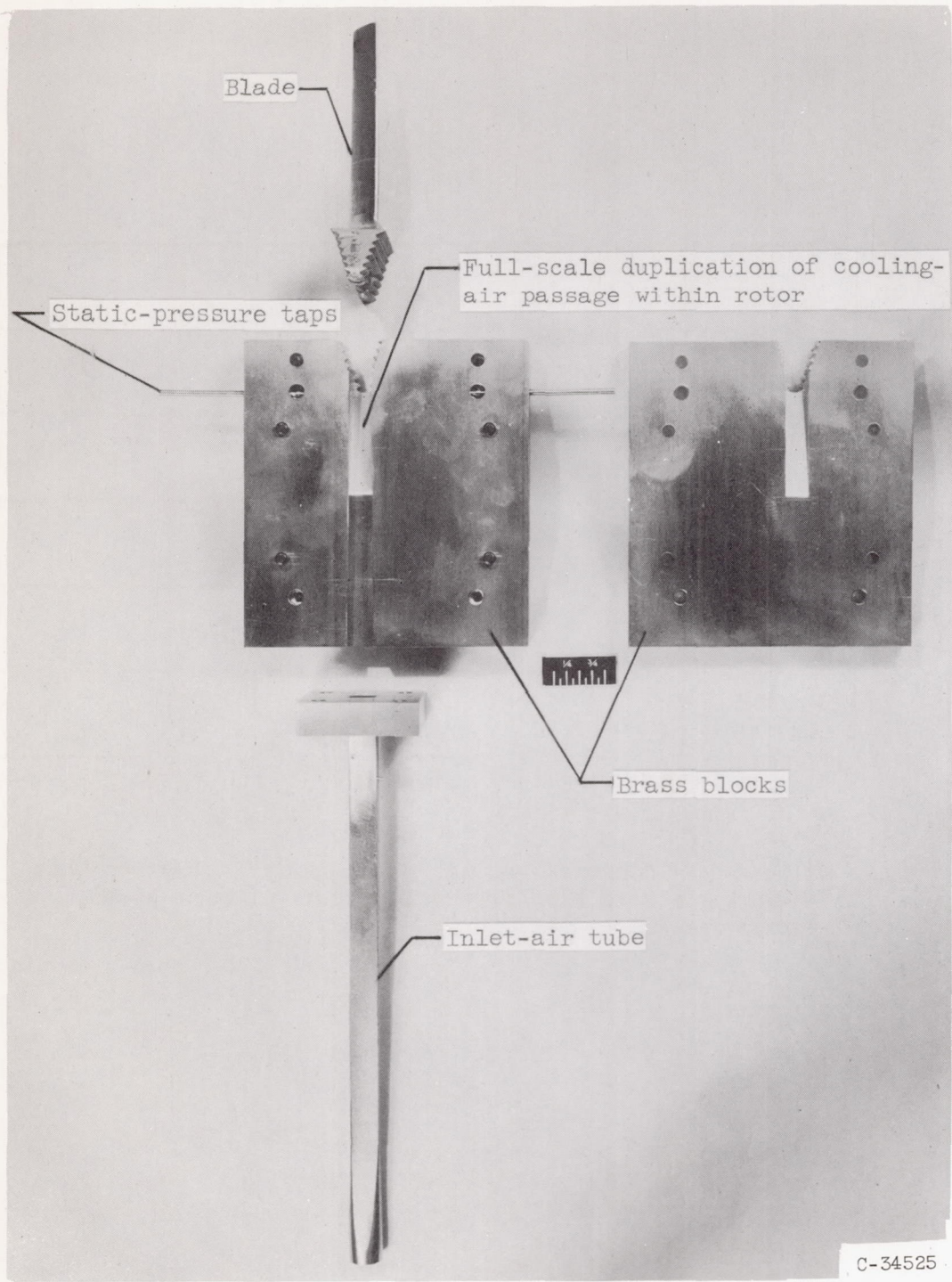
(a) Rotor without inducer vanes.

Figure 10. - Mock-up section of rotor for investigating blade
pressure loss.
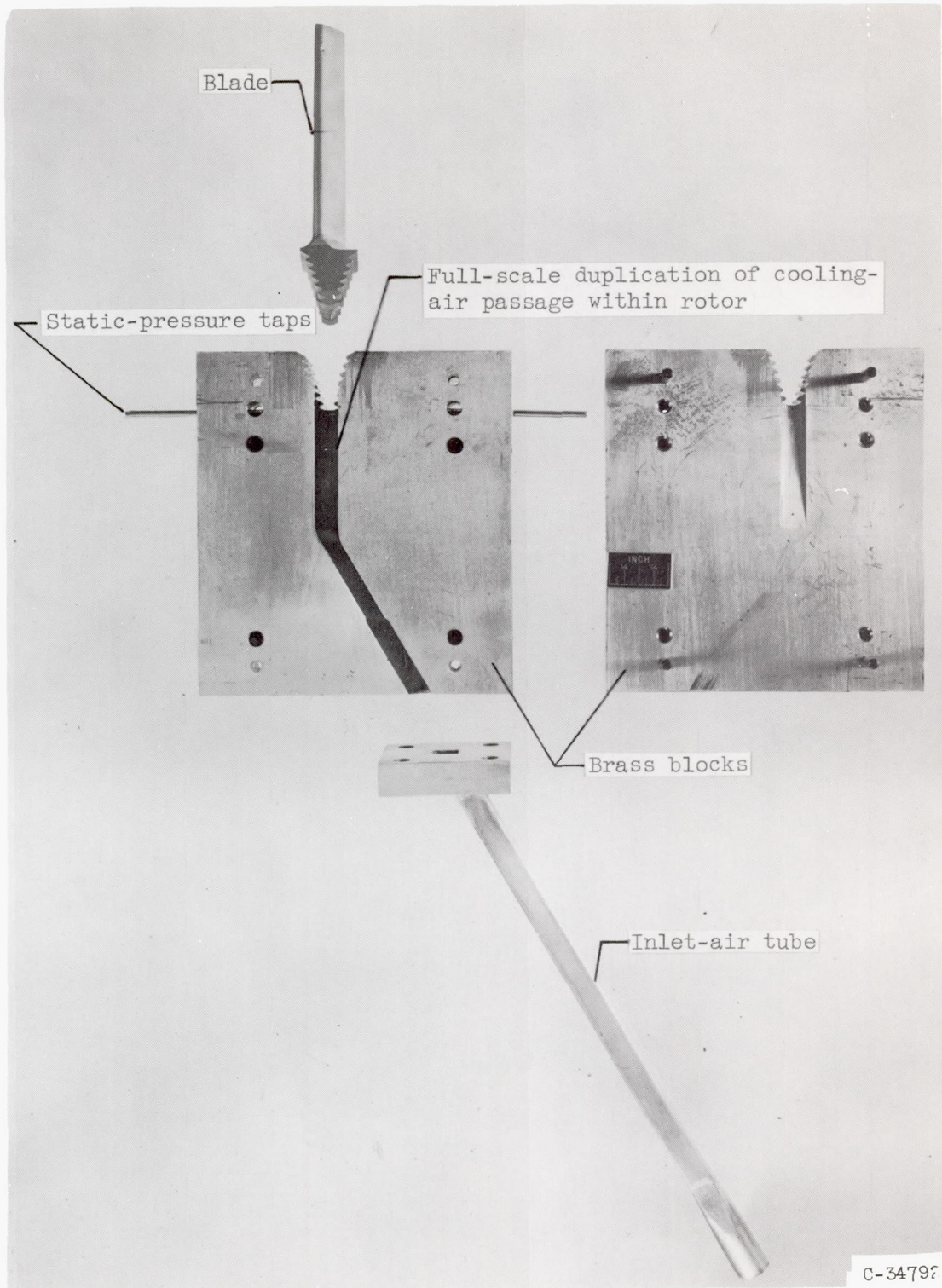
(b) Rotor with inducer section.

Figure 10. - Concluded. Mock-up section of rotor for investigating
blade pressure loss.
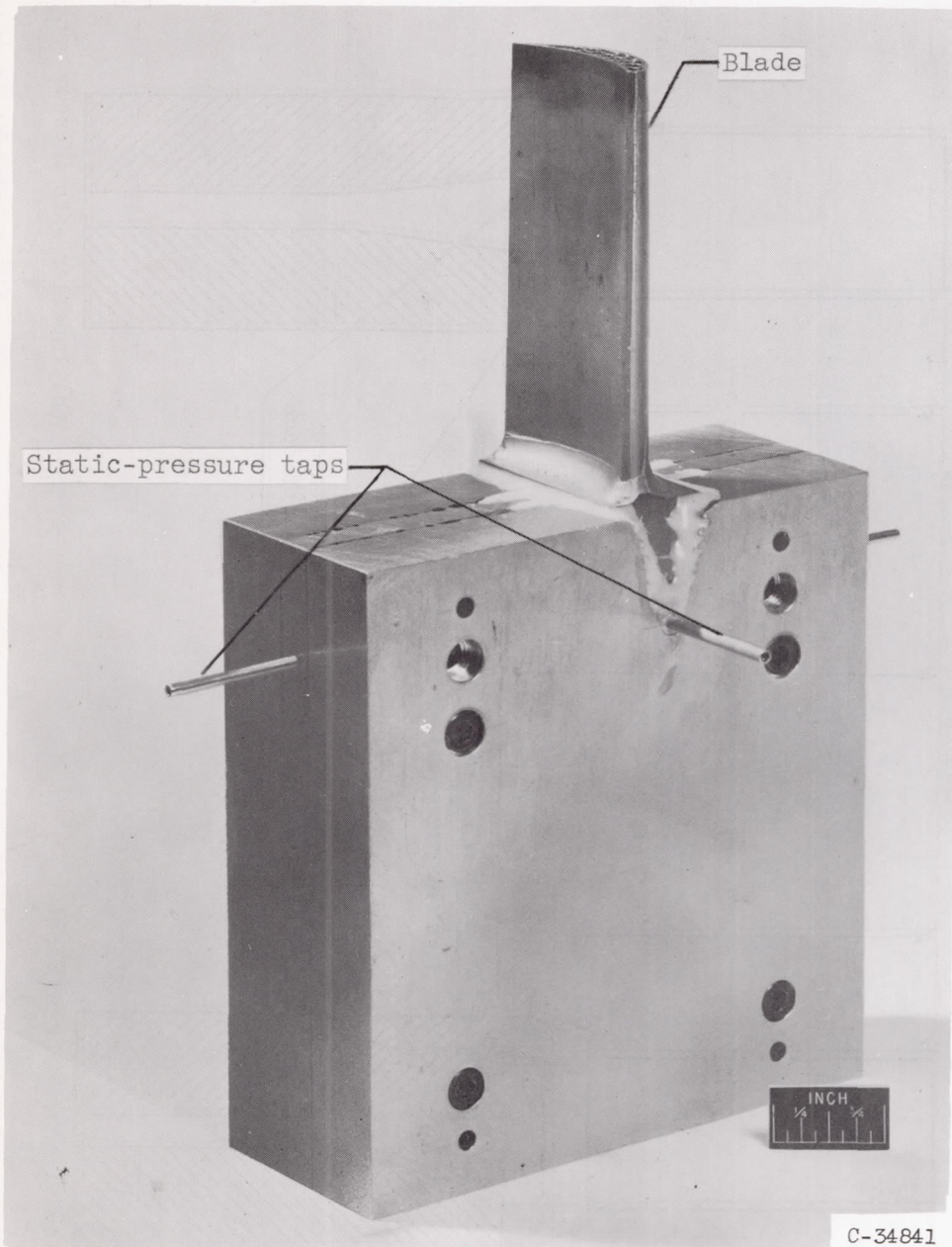
Figure 11. - Assembled mock-up test section of rotor with inducer section.
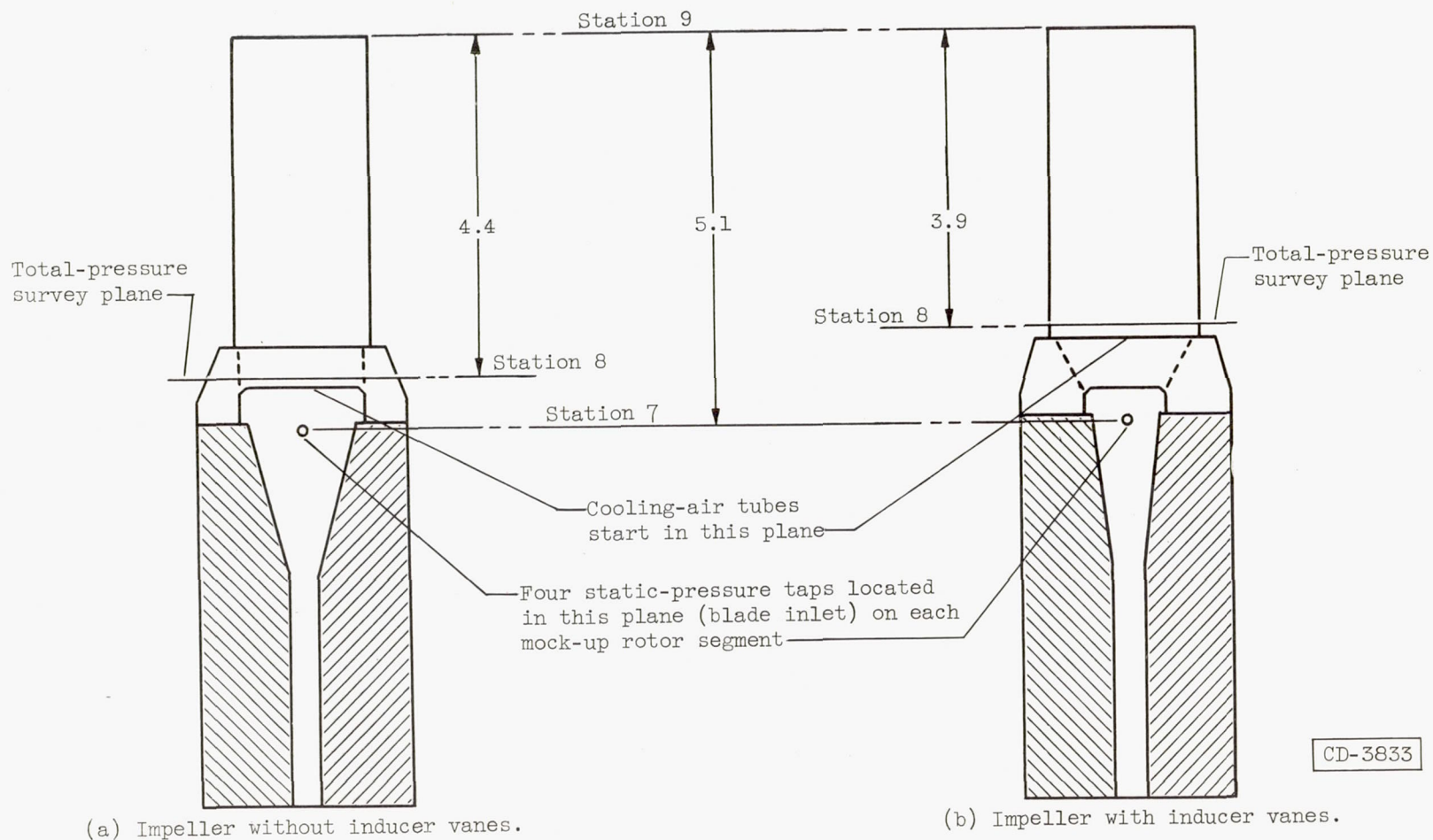
C-34841

(a) Impeller without inducer vanes.

(b) Impeller with inducer vanes.

Figure 12. - Location of pressure instrumentation in mock-up rotor segments. (All dimensions in inches.)
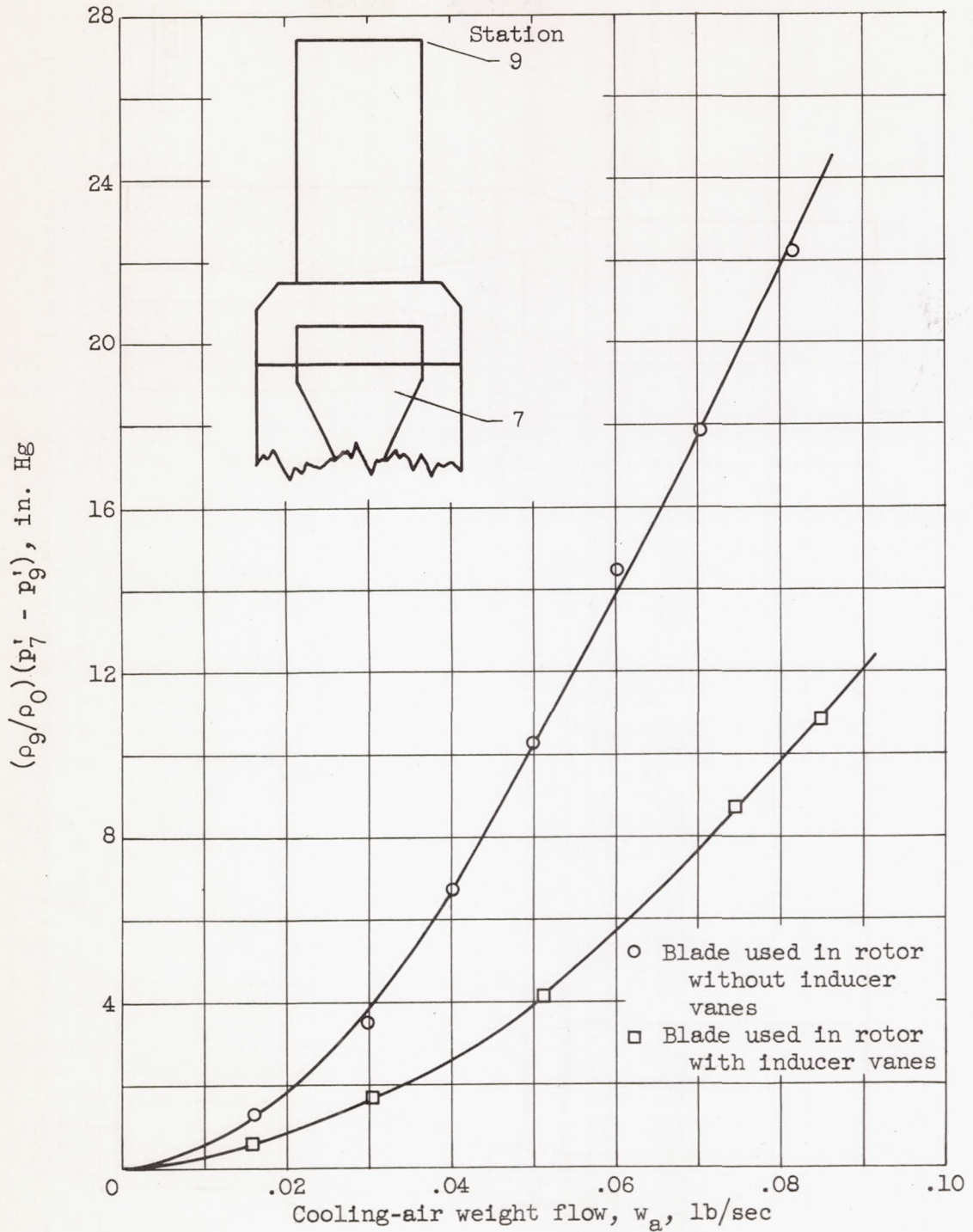
Figure 13. - Blade cooling-air total-pressure loss from
stations 7 to 9 obtained on pressure-loss calibration
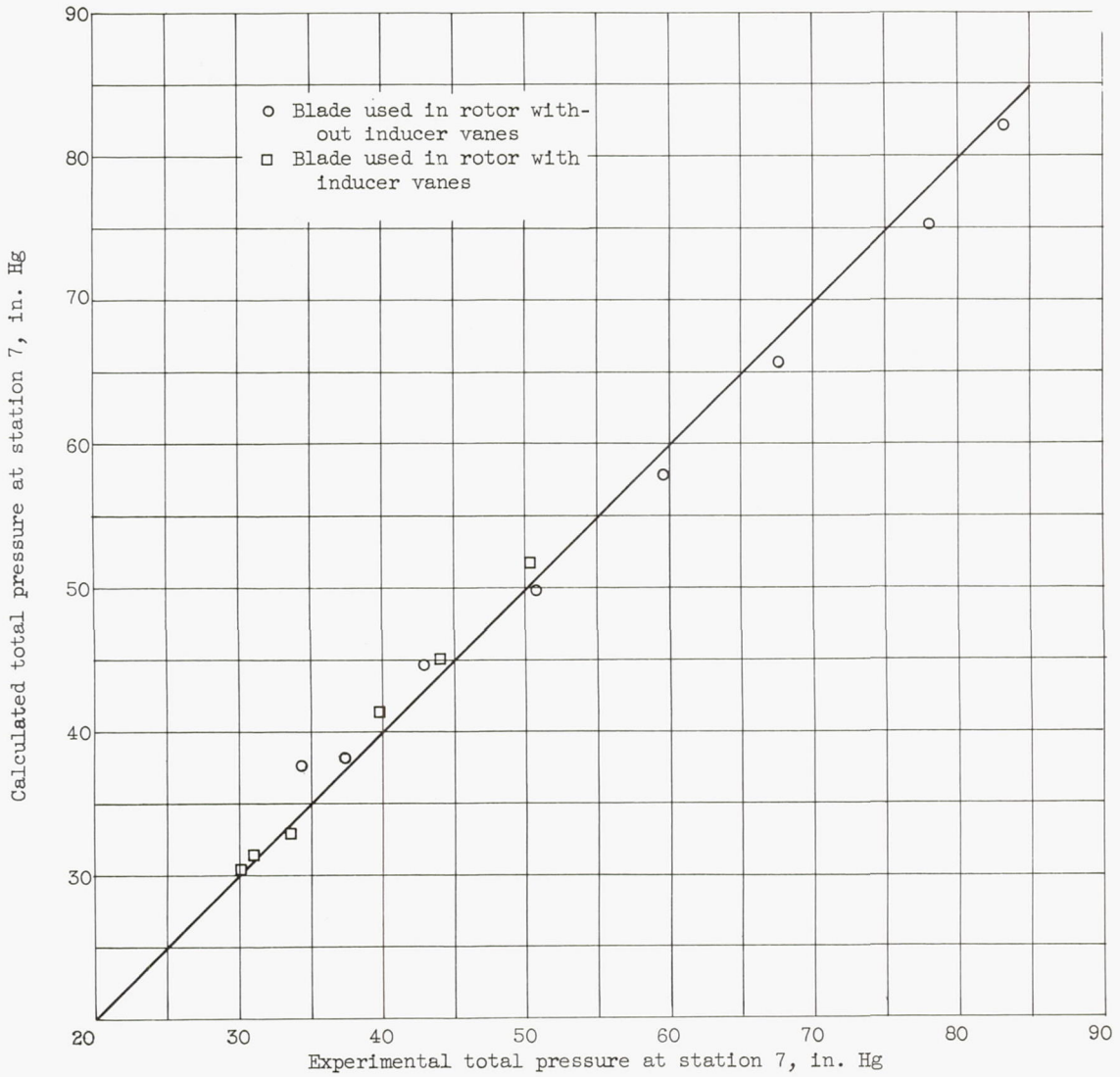rigs.

Figure 14. - Comparison of experimental and calculated cooling-air total pressures at station 7.